

2015

Knots, Skein Theory and q-Series

Mustafa Hajj

Louisiana State University and Agricultural and Mechanical College

Follow this and additional works at: https://digitalcommons.lsu.edu/gradschool_dissertations



Part of the [Applied Mathematics Commons](#)

Recommended Citation

Hajj, Mustafa, "Knots, Skein Theory and q-Series" (2015). *LSU Doctoral Dissertations*. 258.
https://digitalcommons.lsu.edu/gradschool_dissertations/258

This Dissertation is brought to you for free and open access by the Graduate School at LSU Digital Commons. It has been accepted for inclusion in LSU Doctoral Dissertations by an authorized graduate school editor of LSU Digital Commons. For more information, please contact gradetd@lsu.edu.

KNOTS, SKEIN THEORY AND Q-SERIES

A Dissertation

Submitted to the Graduate Faculty of the
Louisiana State University and
Agricultural and Mechanical College
in partial fulfillment of the
requirements for the degree of
Doctor of Philosophy

in

The Department of Mathematics

by

Mustafa Hajj

B.S., Damascus University, 2004

M.S., Jordan University for Science and Technology, 2008

August 2015

Acknowledgments

I would like to express my gratitude to Oliver Dasbach for his advice and patience. I am grateful to Pat Gilmer for many many discussions, ideas and insight. I am also thankful to my topology teachers at Louisiana State University Dan Cohen and Neal Stoltfus. I would like to thank the mathematics department at Louisiana State University for providing excellent study environment. Finally, I would like to thank my family and friends for their encouragement and support.

Table of Contents

Acknowledgments	ii
List of Figures.....	v
Abstract	vii
Chapter 1: Introduction	1
Chapter 2: Background	4
2.1 Preliminaries	4
2.1.1 Alternating and Adequate Links	5
2.2 Skein Theory	6
2.2.1 Skein Maps	10
2.2.2 Quantum Spin Networks	11
2.3 The Colored Jones Polynomial	14
Chapter 3: The Colored Kauffman Skein Relation and the Head and the Tail of the Colored Jones Polynomial	16
3.1 Introduction	16
3.2 The Head and the Tail of the Colored Jones Polynomial for Alter- nating Links	17
3.3 The Colored Kauffman Skein Relation	18
3.4 The Main Theorem	23
Chapter 4: The Bubble Skein Element and the Tail of the Knot 8_5	28
4.1 Introduction	28
4.2 A Recursive Formula for the Bubble Skein Element	31
4.3 The Bubble Expansion Formula	37
4.4 Applications	42
4.4.1 The Theta Graph	42
4.4.2 The Head and the Tail of Alternating Knots	44
Chapter 5: The Tail of a Quantum Spin Network and Roger-Ramanujan Type Identities	55
5.1 Introduction	55
5.2 Background	56
5.2.1 Roger Ramanujan type identities	56
5.3 Existence of the Tail of an Adequate Skein Element	58
5.4 Computing the Tail of a Quantum Spin Network Via Local Skein Relations	60
5.5 Tail Multiplication Structures on Quantum Spin Networks	80

5.6	Applications	83
5.6.1	The Tail of the Colored Jones Polynomial	83
5.6.2	The Tail of the Colored Jones Polynomial and Andrews- Gordon Identities	88
	References	92
	Vita	95

List of Figures

2.1	The three Reidemeister moves.	4
2.2	A and B smoothings	5
2.3	The knot 6_2 , its A -graph on the left and its B -graph on the right	6
2.4	An element in the module of the disk and its mapping to $T_{3,2,2,1}$	12
2.5	The skein element $\tau_{a,b,c}$ in the space $T_{a,b,c}$	12
2.6	The element $\tau_{a,b,c}$	13
2.7	The evaluation of a quantum spin network as an element in $\mathcal{S}(S^2)$	13
2.8	The relative skein module $T_{a,b,c,d}$	14
2.9	A basis of the module $T_{a,b,c,d}$	14
3.1	The n -colored A and B smoothings	21
3.2	n -colored B -state	21
3.3	Adequate and inadequate skein elements. All arcs are colored n	22
3.4	A local picture an adequate skein element	22
3.5	Local view of the skein element $\Upsilon^{(n+1)}(s_-)$	26
4.1	The bubble skein element $\mathcal{B}_{m',n'}^{m,n}(k,l)$	29
4.2	Correspondence between two bases in the module $T_{m,n,n',m'}$	36
4.3	The skein element $\Lambda(m,n,k)$	42
4.4	The knot 4_1 , its A -graph (left). Its reduced A -graph (right)	44
4.5	Obtaining $S_B^{(n)}(D)$ from a knot diagram D	44
4.6	The knot 8_5	45
4.7	The knot Γ	46
4.8	The reduced B -graph for Γ	46
4.9	The skein element $S_B^{(n)}(\Gamma)$	46
5.1	A local picture for $S_B^{(n+1)}(D)$	59

5.2	Expanding $f^{(2n)}$	63
5.3	A crossingless matching that appears in the expansion of $f^{(2n)}$. . .	64
5.4	The graph Γ with a trivalent graph $\tau_{2n,2n,2n}$	80
5.5	The product $[\Gamma_1, \Gamma_2]_1$	81
5.6	The graph Υ (left) and the graph Ξ (right)	82
5.7	The product $[\Upsilon_1, \Upsilon_2]_2$ (left) and the product $[\Xi_1, \Xi_2]_3$ (right)	82
5.8	The graph G_m	87
5.9	The graph $G_{k,l}$	87
5.10	The $(2, f)$ torus knot	89

Abstract

The tail of a sequence $\{P_n(q)\}_{n \in \mathbb{N}}$ of formal power series in $\mathbb{Z}[q^{-1}][[q]]$, if it exists, is the formal power series whose first n coefficients agree up to a common sign with the first n coefficients of P_n . The colored Jones polynomial is link invariant that associates to every link in S^3 a sequence of Laurent polynomials. In the first part of this work we study the tail of the unreduced colored Jones polynomial of alternating links using the colored Kauffman skein relation. This gives a natural extension of a result by Kauffman, Murasugi, and Thistlethwaite regarding the highest and lowest coefficients of Jones polynomial of alternating links. Furthermore, we show that our approach gives a new and natural proof for the existence of the tail of the colored Jones polynomial of alternating links.

In the second part of this work, we study the tail of a sequence of admissible trivalent graphs with edges colored n or $2n$. This can be considered as a generalization of the study of the tail of the colored Jones polynomial. We use local skein relations to understand and compute the tail of these graphs. Furthermore, we consider certain skein elements in the Kauffman bracket skein module of the disk with marked points on the boundary and we use these elements to compute the tail quantum spin networks. We also give product structures for the tail of such trivalent graphs. As an application of our work, we show that our skein theoretic techniques naturally lead to a proof for the Andrews-Gordon identities for the two variable Ramanujan theta function as well to corresponding new identities for the false theta function.

Chapter 1

Introduction

In [7] Dasbach and Lin conjectured that, up to a common sign change, the highest $4(n+1)$ (the lowest resp.) coefficients of the n^{th} unreduced colored Jones polynomial $\tilde{J}_{n,L}(A)$ of an alternating link L agree with the first $4(n+1)$ coefficients of the polynomial $\tilde{J}_{n+1,L}(A)$ for all n . This gives rise to two power series with integer coefficients associated with the alternating link L called the head and the tail of the colored Jones polynomial. The existence of the head and tail of the colored Jones polynomial of adequate links was proven by Armond in [4] using skein theory. Independently, this was shown by Garoufalidis and Le for alternating links using R -matrices [8] and generalized to higher order stability of the coefficients of the colored Jones polynomial.

Let L be an alternating link and let D be a reduced link diagram of L . Write $S_A(D)$ to denote the A -smoothing state of D , the state obtained by replacing each crossing by an A -smoothing. The state $S_B(D)$ of D is defined similarly. Using the Kauffman skein relation Kauffman [17], Murasugi [28], and Thistlethwaite [33] showed that the A state (respectively the B state) realizes the highest (respectively the lowest) coefficient of the Jones polynomial of an alternating link. In chapter 2, we extend this result to the colored Jones polynomial by using *the colored Kauffman skein relation* 4.2. We show that the n -colored A state and the n -colored B state realize the highest and the lowest $4n$ coefficients of the n^{th} unreduced colored Jones polynomial of an alternating link. Furthermore we show that this gives a natural layout to prove the stability of the highest and lowest coefficients of the

colored Jones polynomial of alternating links. In other words we prove that the head and the tail of the colored Jones polynomial exist.

Let $S_B^{(n)}(D)$ be the skein element obtained from $S_B(D)$ by decorating each circle in this state with the n^{th} Jones-Wenzl idempotent and replacing each place where we had a crossing in D with the $(2n)^{th}$ projector. It was proven in [3] that for an adequate link L the first $4(n+1)$ coefficients of n^{th} unreduced colored Jones polynomial coincide with the first $4(n+1)$ coefficients of the skein element $S_B^{(n)}(D)$. In chapter 3, we study a certain skein element, called *the bubble skein element*, in the relative Kauffman bracket skein module of the disk with some marked points, and expand this element in terms of linearly independent elements of this module. Then we use the bubble skein element in the study of the tail of 8_5 considering the skein element $S_B^{(n)}(D)$ obtained from an alternating diagram of 8_5 . The knot 8_5 is the first knot on the knot table whose tail could not be determined directly by the techniques developed [3].

In chapter 4, we extend the study of the tail of the colored Jones polynomial that we started in the previous chapter to study the tail of quantum spin networks. A quantum spin network is a banded trivalent graph with edges labeled by non-negative integers, also called the colors of the edges, and the three edges meeting at a vertex satisfy some admissibility conditions. Skein theoretic techniques have been used in [3] and [4] to understand the head and tail of an adequate link. It was proven in [3] that for an adequate link L the first $4(n+1)$ coefficients of n^{th} unreduced colored Jones polynomial coincide with the first $4(n+1)$ coefficients of the evaluation in $\mathcal{S}(S^2)$ of a certain skein element in S^2 . We demonstrate here that this skein element can be realized as quantum spin network obtained from the

link diagram D . Hence, studying the tail of the colored Jones polynomial can be reduced to studying the tail of these quantum spin networks. Our method to study the tail of such graphs relies mainly on adapting various skein theoretic identities to new ones that can in turn be used to compute and understand the tail of such graphs. We use this structure to give natural product structures on the tail of quantum spin networks.

The q -series obtained from knots in this way appear to be connected to classical number theoretic identities. Hikami [14] realized that that Rogers-Ramanujan identities appear in the study of the colored Jones polynomial of torus knots. In [4] Armond and Dasbach calculate the head and the tail of the colored Jones polynomial via multiple methods and use these computations to prove number theoretic identities. In chapter 4, we show that the skein theoretic techniques we developed herein can be also used to prove classical identities in number theory. In particular we use skein theory to prove the Andrews-Gordon identities for the two variable Ramanujan theta function, as well as corresponding new identities for the false theta function.

Chapter 2

Background

2.1 Preliminaries

A *knot* in the 3-sphere S^3 is a piecewise-linear one-to-one mapping $f : S^1 \longrightarrow S^3$. A *link* in S^3 is a finite ordered collection of knots, called the components of the link, that do not intersect each other. Two links are considered to be equivalent if they are ambient isotopic. A *link diagram* of a link L is a projection of L on S^2 such that this projection has a finite number of nontangential intersection points (called *crossings*), each of which is coming from exactly two points of the link L . We usually draw a small break in the projection of the lower strand to indicate that it crosses under the other strand. Reidemeister's theorem asserts that two links are ambient isotopic if and only if their diagrams can be transformed into the other by a finite sequence of *Reidemeister moves*. See Figure 2.1.

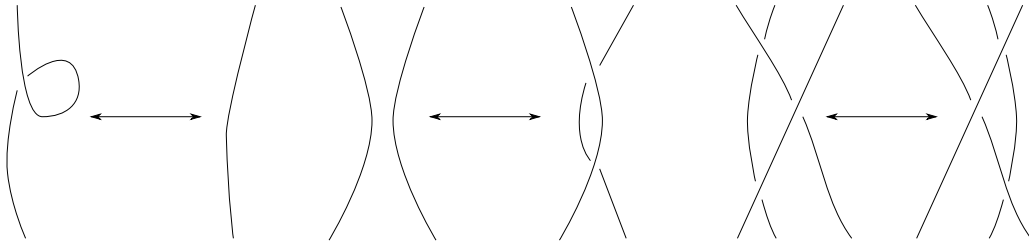


FIGURE 2.1. The three Reidemeister moves.

A *framed link* is a link together with a smooth section of the normal bundle over the link called a *framing*. Framed links are also considered up to ambient isotopy. In this thesis we will deal mostly with framed links. We will assume that link diagrams are equipped with *blackboard framing*. Any diagram of a link L gives rise to a framing of L by taking a nonzero vector field that is everywhere parallel to the projection plane of the diagram. This framing is called the blackboard

framing. Any arbitrary framed link can be represented by a link diagram with the blackboard framing. Appropriate insertion of curls in the diagram adjusts the blackboard framing of the diagram so that one can realize any framing.

2.1.1 Alternating and Adequate Links

Let L be a link in S^3 and let D be an alternating knot diagram of L . For any crossing in D there are two ways to smooth this crossing, the A -smoothing and the B -smoothing. See Figure 2.2.

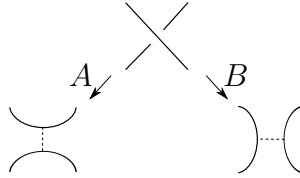


FIGURE 2.2. A and B smoothings

We replace a crossing with a smoothing together with a dashed line joining the two arcs. After applying a smoothing to each crossing in D we obtain a planar diagram consisting of a collection of disjoint circles in the plane. We call this diagram a *state* for the diagram D . The A -smoothing state, obtained from D by replacing every crossing by an A smoothing, and the B -smoothing state for D are of particular importance for us. Write $S_A(D)$ and $S_B(D)$ to denote the A smoothing and B smoothing states of D respectively. For each state S of a link diagram D one can associate a graph obtained by replacing each circle of S by a vertex and each dashed link by an edges. In particular we are interested in the graphs obtained by the A -smoothing state and the B -smoothing state of the diagram D . We will denote these two graphs by $A(D)$ and $B(D)$ respectively.

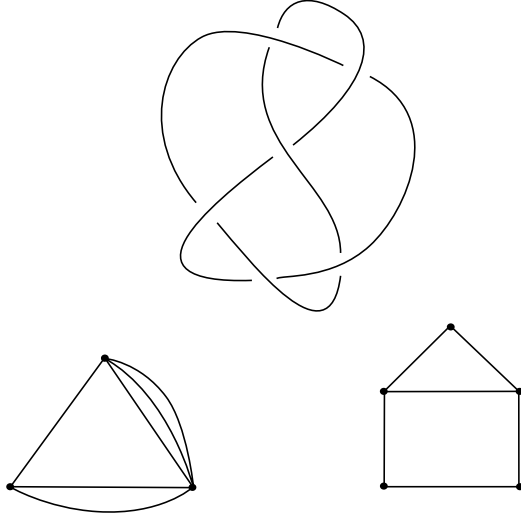


FIGURE 2.3. The knot 6_2 , its A -graph on the left and its B -graph on the right

Recall that a link diagram is *alternating* if as we travel along the link, from any starting point, the crossings alternating between under and over crossings. A link is called alternating if it possesses such a diagram. The following definition can be considered as a generalization of the alternating links.

Definition 2.1. *A link diagram D is called A -adequate (B -adequate, respectively) if there are no loops in the graph $A(D)$ (the graph $B(D)$, respectively). A link diagram D is called adequate if it is both A -adequate and B -adequate.*

It is known that a reduced alternating link diagram is adequate. See for example [22].

2.2 Skein Theory

In this section we review the fundamentals of the Kauffman Bracket Skein Modules and introduce the skein modules that will be used for our purpose. Furthermore, we discuss the recursive definition of Jones-Wenzl idempotent and recall some of its basic properties. For more details about linear skein theory associated with the Kauffman Bracket, see [19], [22], and [29].

Definition 2.2. (*J. Przytycki [29] and V. Turaev [34]*) Let M be an oriented 3-manifold. Let \mathbf{R} be a commutative ring with identity and a fixed invertable element A . Let \mathcal{L}_M be the set of isotopy classes of framed links in M including the empty link. Let $\mathbf{R}\mathcal{L}_M$ be the free \mathbf{R} -module generated by the set \mathcal{L}_M . Let $K(M)$ be the smallest submodule of $\mathbf{R}\mathcal{L}_M$ that is generated by all expressions of the form

$$(1) \quad \left(\begin{array}{c} \diagup \diagdown \\ \diagdown \diagup \end{array} - A \right) \left(-A^{-1} \begin{array}{c} \cup \\ \cap \end{array} \right), \quad (2) \quad L \sqcup \bigcirc + (A^2 + A^{-2})L.$$

where $L \sqcup \bigcirc$ consists of a framed link L in M and the trivial framed knot \bigcirc . The Kauffman bracket skein module, $\mathcal{S}(M; \mathbf{R}, A)$, is defined to be the quotient module $\mathcal{S}(M; \mathbf{R}, A) = \mathbf{R}\mathcal{L}_M / K(M)$.

A relative version of the Kauffman bracket skein module can be defined when M has a boundary. The definition is extended as follows. We specify a finite (possibly empty) set of framed points x_1, x_2, \dots, x_{2n} on the boundary of M . A band is a surface that is homeomorphic to $I \times I$. An element in the set \mathcal{L}_M is an isotopy class of an oriented surface embedded into M and decomposed into a union of finite number of framed links and bands joining the designated boundary points. Let $K(M)$ be the smallest submodule of $\mathbf{R}\mathcal{L}_M$ that is generated by Kauffman relations specified above. The Kauffman bracket skein module is defined to be the quotient module $\mathcal{S}(M; \mathbf{R}, A, \{x_i\}_{i=1}^{2n}) = \mathbf{R}\mathcal{L}_M / K(M)$. The relative Kauffman bracket skein module depends only on the distribution of the points $\{x_i\}_{i=1}^{2n}$ among the different connected components of ∂M and it does not depend on the exact position of the points $\{x_i\}_{i=1}^{2n}$. In particular, if ∂M is connected then the definition of the relative Kauffman bracket skein module is independent of the choice of the exact position of the points $\{x_i\}_{i=1}^{2n}$. For more details see [29] and [30].

When the manifold M is homeomorphic to $F \times [0, 1]$, where F is a surface with a finite set of points (possibly empty) in its boundary ∂F , one could define the (relative) Kauffman bracket skein module of F . In this case one considers an appropriate version of link diagrams in F instead of framed links in M . The isomorphism between $\mathcal{S}(M; \mathbf{R}, A)$ and $\mathcal{S}(F; \mathbf{R}, A)$ that sends a framed link to its link diagram will be used to identify these two skein modules.

We will work with the skein module of the sphere $\mathcal{S}(S^2; \mathbf{R}, A)$. This skein module is freely generated by one generator. Let D be any diagram in S^2 . Using the definition of the normalized Kauffman bracket [17], we can write $D = \langle D \rangle \phi$ in $\mathcal{S}(S^2; \mathbf{R}, A)$, where ϕ denotes the empty link. This provides an isomorphism $\langle \rangle: \mathcal{S}(S^2; \mathbf{R}, A) \rightarrow \mathbf{R}$, induced by sending D to $\langle D \rangle$. In particular this isomorphism sends the empty link ϕ in $\mathcal{S}(S^2; \mathbf{R}, A)$ to the identity in \mathbf{R} . We will also work with the relative skein module $\mathcal{S}([0, 1] \times [0, 1]; \mathbf{R}, A, \{x_i\}_{i=1}^{2n})$, where the rectangular disk $[0, 1] \times [0, 1]$ has n designated points $\{x_i\}_{i=1}^n$ on the top edge, where $x_i = (1, \frac{i}{n+1})$ for $1 \leq i \leq n$, and n designated points on the bottom edge $\{x_i\}_{i=n+1}^{2n}$, where $x_i = (0, \frac{i-n}{n+1})$ for $n+1 \leq i \leq 2n$. As we mentioned above, the relative skein module $\mathcal{S}([0, 1] \times [0, 1]; \mathbf{R}, A, \{x_i\}_{i=1}^{2n})$ does not depend on the exact position of the points $\{x_i\}_{i=1}^{2n}$. However, we are making a choice for the position of the points here because we will define an algebra structure on $\mathcal{S}([0, 1] \times [0, 1]; \mathbf{R}, A, \{x_i\}_{i=1}^{2n})$ where the position of these points is required. This relative skein module can be thought of as the \mathbf{R} -module generated by all (n, n) -tangle diagrams in $[0, 1] \times [0, 1]$ modulo the Kauffman relations. In fact the module $\mathcal{S}([0, 1] \times [0, 1]; \mathbf{R}, A, \{x_i\}_{i=1}^{2n})$ is a free \mathbf{R} -module on $\frac{1}{n+1} \binom{2n}{n}$ free generators. For a proof of this fact see [29]. The relative skein module $\mathcal{S}([0, 1] \times [0, 1]; \mathbf{R}, A, \{x_i\}_{i=1}^{2n})$ admits a multiplication given by juxtaposition of two diagrams in $[0, 1] \times [0, 1]$. More precisely, let D_1

and D_2 be two diagrams in $[0, 1] \times [0, 1]$ such that ∂D_j , where $j = 1, 2$, consists of the points $\{x_i\}_{i=1}^{2n}$ specified above. Define $D_1.D_2$ to be the diagram in $[0, 1] \times [0, 1]$ obtained by attaching D_1 on the top of D_2 and then compress the result to $[0, 1] \times [0, 1]$. This multiplication on diagrams extends to a well-defined multiplication on isotopy classes of diagrams in $[0, 1] \times [0, 1]$. Finally it extends by linearity to a multiplication on $\mathcal{S}([0, 1] \times [0, 1]; \mathbf{R}, A, \{x_i\}_{i=1}^{2n})$. With this multiplication $\mathcal{S}([0, 1] \times [0, 1]; \mathbf{R}, A, \{x_i\}_{i=1}^{2n})$ is an associative algebra over \mathbf{R} known as the n^{th} Temperley-Lieb algebra TL_n . For each n there exists an idempotent $f^{(n)}$ in TL_n that plays a central role in the Witten-Reshetikhin-Turaev Invariants for $SU(2)$. See [19], [21], and [32]. The idempotent $f^{(n)}$, known as the n^{th} Jones-Wenzl idempotent, was discovered by Jones [16] and it has a recursive formula due to Wenzl [35]. We will use this recursive formula to define $f^{(n)}$. Further, we will adapt a graphical notation for $f^{(n)}$ which is due Lickorish [20]. In this graphical notation one thinks of $f^{(n)}$ as an empty box with n strands entering and n strands leaving the opposite side. The Jones-Wenzl idempotent is defined by:

$$\begin{array}{c} \begin{array}{|c|} \hline n \\ \hline \end{array} \begin{array}{|c|} \hline n-1 \\ \hline \end{array} \begin{array}{|c|} \hline 1 \\ \hline \end{array} \\ \hline \end{array} = \begin{array}{c} \begin{array}{|c|} \hline n-1 \\ \hline \end{array} \begin{array}{|c|} \hline 1 \\ \hline \end{array} \\ \hline \end{array} - \left(\frac{\Delta_{n-2}}{\Delta_{n-1}} \right) \begin{array}{c} \begin{array}{|c|} \hline n-1 \\ \hline \end{array} \begin{array}{|c|} \hline 1 \\ \hline \end{array} \\ \hline \end{array} \begin{array}{c} \begin{array}{|c|} \hline n-2 \\ \hline \end{array} \begin{array}{|c|} \hline 1 \\ \hline \end{array} \\ \hline \end{array} \begin{array}{c} \begin{array}{|c|} \hline n-1 \\ \hline \end{array} \begin{array}{|c|} \hline 1 \\ \hline \end{array} \\ \hline \end{array} \begin{array}{c} \begin{array}{|c|} \hline 1 \\ \hline \end{array} \begin{array}{|c|} \hline 1 \\ \hline \end{array} \\ \hline \end{array} \quad (2.1)$$

where

$$\Delta_n = (-1)^n \frac{A^{2(n+1)} - A^{-2(n+1)}}{A^2 - A^{-2}}.$$

The polynomial Δ_n is related to $[n+1]$, the $(n+1)^{th}$ quantum integer, by $\Delta_n = (-1)^n [n+1]$. It is common to use the substitution $a = A^2$ when one works with quantum integers.

We assume that $f^{(0)}$ is the empty diagram. The Jones-Wenzl idempotent satisfies

$$\Delta_n = \text{circle with } n \text{ strands and a box} \quad \begin{array}{c} n \quad m \\ \text{box} \\ m+n \end{array} = \begin{array}{c} \text{box} \\ m+n \end{array}, \quad \begin{array}{c} n \quad m \\ \text{box with 1 strand} \\ m+n+2 \end{array} = 0, \quad (2.2)$$

$$(1) \quad \Delta_n = \text{circle with } n \text{ strands and a box} \quad (2) \quad \begin{array}{c} n \quad m \\ \text{box} \\ m+n \end{array} = \begin{array}{c} \text{box} \\ m+n \end{array} \quad (2.3)$$

and

$$(1) \quad \begin{array}{c} n \\ \text{circle with } m \text{ strands and a box} \end{array} = \frac{\Delta_{m+n}}{\Delta_n} \begin{array}{c} n \\ \text{box} \end{array}, \quad (2) \quad \begin{array}{c} i \quad j \\ \text{crossing} \\ i+j \end{array} = A^{-ij} \begin{array}{c} \text{box} \\ i+j \end{array} \quad (2.4)$$

In this thesis \mathbf{R} will be $\mathbb{Q}(A)$, the field generated by the indeterminate A over the rational numbers. Before we introduce any other skein modules we talk briefly about linear maps between skein modules.

2.2.1 Skein Maps

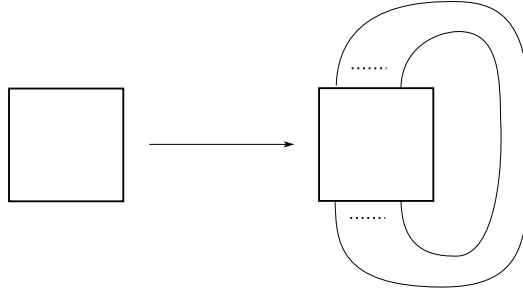
We can relate various skein modules by linear maps induced from maps between surfaces. Let F and F' be two oriented surfaces with marked points on their boundaries. A *wiring* is an orientation preserving embedding between F and F' along with a fixed *wiring diagram* of arcs and curves in $F' - F$ such that the boundary points of the arcs consists of all the marked points of F and F' . Any diagram D in F induces a diagram $\mathcal{W}(D)$ in F' by extending D by wiring diagram. A wiring

W of F into F' induces the module homomorphism

$$\mathcal{S}(W) : \mathcal{S}(F) \longleftrightarrow \mathcal{S}(F')$$

defined by $D \longrightarrow W(D)$ for any D diagram in F . For more details see [?].

Example 2.3. Consider the square $I \times I$ with n marked points on the top edge and n marked points on the bottom edge. Embed $I \times I$ in S^2 and join the n points on the top edge to the n points on the bottom edge by parallel arcs as follows:



For each n , this wiring induces a module homomorphism:

$$tr_n : TL_n \longrightarrow \mathcal{S}(S^2)$$

This map is usually called the Markov trace on TL_n .

2.2.2 Quantum Spin Networks

Before giving the definition of quantum spin network we will need to introduce a few relative skein modules. Consider the relative skein module of the disk with $a_1 + \dots + a_m$ marked points on the boundary. We are interested in a submodule of this module constructed as follows. Partition the set of the $a_1 + \dots + a_m$ points into m sets of a_1, \dots, a_{m-1} and a_m points respectively. At each cluster of these points we place an appropriate idempotent, i.e. the one whose color matches the cardinality of this cluster. We will denote this relative skein module by T_{a_1, \dots, a_m} . Hence an element in T_{a_1, \dots, a_m} is obtained by taking an element in the module of the disk with $a_1 + \dots + a_m$ marked points and then adding the idempotents $f^{(a_1)}, \dots, f^{(a_m)}$

on the outside of the disk. Figure 2.4 shows an element in the Kauffman bracket skein module of the disk with $3 + 2 + 2 + 1$ marked points on the boundary and the corresponding element in the space $T_{3,2,2,1}$.

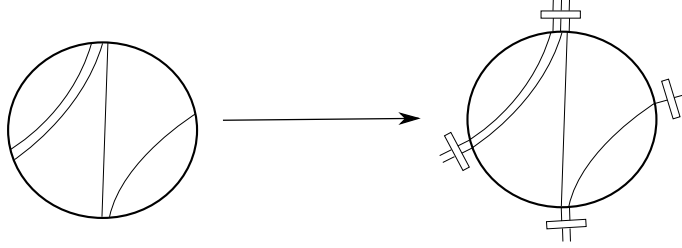


FIGURE 2.4. An element in the module of the disk and its mapping to $T_{3,2,2,1}$.

Of particular interest are the spaces $T_{a,b}$, $T_{a,b,c}$ and $T_{a,b,c,d}$. The properties of the Jones-Wenzl projector imply that the space $T_{a,b}$ is zero dimensional when $a \neq b$ and one dimensional when $a = b$, spanned by $f^{(a)}$. Similarly, $T_{a,b,c}$ is either zero dimensional or one dimensional. The space $T_{a,b,c}$ is one dimensional if and only if the element $\tau_{a,b,c}$ shown in Figure 2.5 exists. This occurs when one has non-negative integers x, y and z such that the following three equations are satisfied

$$a = x + y, \quad b = x + z, \quad c = y + z. \quad (2.5)$$

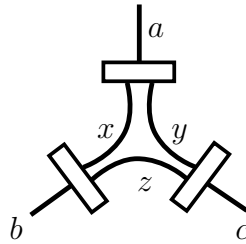


FIGURE 2.5. The skein element $\tau_{a,b,c}$ in the space $T_{a,b,c}$

When $\tau_{a,b,c}$ exists we will refer to the outside colors of $\tau_{a,b,c}$ by the colors a, b and c and to the inside colors of $\tau_{a,b,c}$ by the colors x, y and z . The following definition characterizes the existence of the element $\tau_{a,b,c}$ in terms of the outside colors.

Definition 2.4. A triple of colors (a, b, c) is admissible if $a + b + c \equiv 0 \pmod{2}$ and $a + b \geq c \geq |a - b|$.

Note that if the triple (a, b, c) is admissible, then writing $x = (a + b - c)/2$, $y = (a + c - b)/2$, and $z = (b + c - a)/2$ we have that x, y and z satisfy the equations 2.5. If the triple (a, b, c) is not admissible then the space $T_{a,b,c}$ is zero dimensional. The fact that the inside colors are determined by the outside colors allows us to replace $\tau_{a,b,c}$ by a trivalent graph as follows:

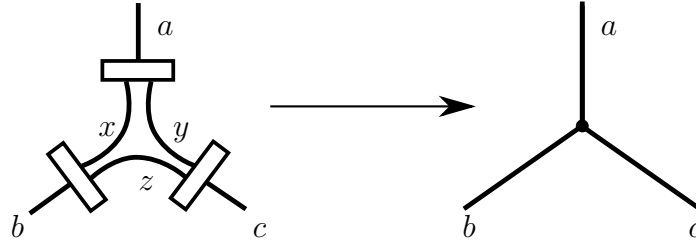


FIGURE 2.6. The element $\tau_{a,b,c}$

This motivates the following definition.

Definition 2.5.

A quantum spin network in S^2 is an embedded trivalent graph in $S^2 \times I$ with edges labeled by non-negative integers and the labels of the edges meeting at a vertex satisfy the admissibility condition. Let Γ be a quantum spin network in S^2 . The Kauffman bracket evaluation of Γ is defined to be bracket of the expansion of Γ after replacing every edge labeled n by the projector $f^{(n)}$ and every vertex labeled (a, b, c) by the skein element $\tau_{a,b,c}$. See Figure 2.7.

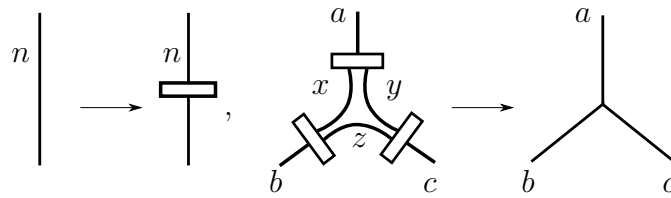


FIGURE 2.7. The evaluation of a quantum spin network as an element in $\mathcal{S}(S^2)$.

We assume that a diagram represent the zero element in the module if it has a strand labeled by a negative number. The last relative Kauffman bracket skein module that we need here is the module $T_{a,b,c,d}$, see Figure 2.8.

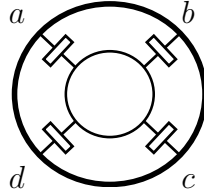


FIGURE 2.8. The relative skein module $T_{a,b,c,d}$

This module is free on the set of generators given in Figure 2.9. Here i runs over all possible positive integers such that (a, b, i) and (c, d, i) are admissible.

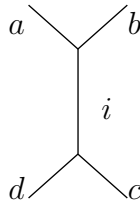


FIGURE 2.9. A basis of the module $T_{a,b,c,d}$

2.3 The Colored Jones Polynomial

In 1980s a vast family of new knot invariants, called quantum invariants were discovered and later extended to invariants of 3-manifolds. The first quantum invariant was discovered by Jones in [15]. The Jones polynomial is a Laurent polynomial knot invariant in the variable q with integer coefficients. The Jones polynomial generalizes to an invariant $J_{K,V}^{\mathfrak{g}}(q) \in \mathbb{Z}[q^{\pm 1}]$ of a zero-framed knot K colored by a representation V of a simple Lie algebra \mathfrak{g} , and normalized so that $J_{O,V}^{\mathfrak{g}}(q) = 1$, where O denotes the zero-framed unknot. The invariant $J_{K,V}^{\mathfrak{g}}(q)$ is called the quantum invariant of the knot K associated with the simple Lie algebra \mathfrak{g} and the representation V . The Jones polynomial corresponds to the 2- dimensional irreducible representation of $\mathfrak{sl}(2, \mathbb{C})$ and the n^{th} colored Jones polynomial, denoted by

$J_{n,K}(q)$, is the quantum invariant associated with the $n+1$ -dimensional irreducible representation of $\mathfrak{sl}(2, \mathbb{C})$.

Another version of the colored Jones polynomial is the *unreduced colored Jones polynomial*. Let L be zero-framed framed link in S^3 . The n^{th} unreduced colored Jones polynomial of a link L is obtained by decorating every component of L , according to its framing, by the n^{th} Jones-Wenzl idempotent and consider this decorated framed link as an element of $\mathcal{S}(S^3)$. The two versions of the colored Jones polynomial are related by a change of variable and a shift the index by 1. In what follows we assume $A^4 = q$.

In the next chapter we start studying the highest and the lowest coefficients of the colored Jones polynomial using mainly the skein theoretic definition of the unreduced colored Jones polynomial.

Chapter 3

The Colored Kauffman Skein Relation and the Head and the Tail of the Colored Jones Polynomial

3.1 Introduction

In [7] Dasbach and Lin conjectured that, up to a common sign change, the highest $4(n+1)$ (the lowest resp.) coefficients of the n^{th} unreduced polynomial $\tilde{J}_{n,L}(A)$ of an alternating link L agree with the first $4(n+1)$ coefficients of the polynomial $\tilde{J}_{n+1,L}(A)$ for all n . This gives rise to two power series with integer coefficients associated with the alternating link L called the head and the tail of the colored Jones polynomial. The existence of the head and tail of the colored Jones polynomial of adequate links was proven by Armond in [4] using skein theory. Independently, this was shown by Garoufalidis and Le for alternating links using R -matrices [8] and generalized to higher order tails.

Let L be an alternating link and let D be a reduced link diagram of L . Write $S_A(D)$ to denote the A -smoothing state of D , the state obtained by replacing each crossing by an A -smoothing. The state $S_B(D)$ of D is defined similarly. Using the Kauffman skein relation Kauffman [17] showed that the A state (respectively the B state) realizes the highest (respectively the lowest) coefficient of the Jones polynomial of an alternating link. In this chapter we extend this result to the colored Jones polynomial by using *the colored Kauffman skein relation* 4.2. We show that the n -colored A state and the n -colored B state realize the highest and the lowest $4n$ coefficients of the n^{th} unreduced colored Jones polynomial of an alternating link. Furthermore we show that this gives a natural layout to prove the

stability of the highest and lowest coefficients of the colored Jones polynomial of alternating links. In other words we prove that the head and the tail of the colored Jones polynomial exist.

3.2 The Head and the Tail of the Colored Jones Polynomial for Alternating Links

Let $P_1(q)$ and $P_2(q)$ be elements in $\mathbb{Z}[q^{-1}][[q]]$, we write $P_1(q) \doteq_n P_2(q)$ if their first n coefficients agree up to a sign.

Definition 3.1. *Let $\mathcal{P} = \{P_n(q)\}_{n \in \mathbb{N}}$ be a sequence of formal power series in $\mathbb{Z}[q^{-1}][[q]]$. The tail of the sequence \mathcal{P} - if it exists - is the formal power series $T_{\mathcal{P}}(q)$ in $\mathbb{Z}[[q]]$ that satisfies*

$$T_{\mathcal{P}}(q) \doteq_n P_n(q), \text{ for all } n \in \mathbb{N}.$$

Observe that the tail of the sequence $\mathcal{P} = \{P_n(q)\}_{n \in \mathbb{N}}$ exists if and if only if $P_n(q) \doteq_n P_{n+1}(q)$ for all n . We will need the definition of the minimal degree of such formal power series. If $p \in \mathbb{Z}[q^{-1}][[q]]$ then we will denote by $m(p)$ to the minimal degree of p .

Remark 3.2. *Consider the sequence $\{f_n(q)\}_{n \in \mathbb{N}}$ where $f_n(q)$ is a rational function in $\mathbb{Q}(q)$. Every rational function in $\mathbb{Q}(q)$ can be represented uniquely as an element $\mathbb{Z}[q^{-1}][[q]]$. Using this convention one can study the tail of the sequence $\{f_n(q)\}_{n \in \mathbb{N}}$. Furthermore, this can be used to define the minimal degree of a rational function.*

Let $\mathcal{D} = \{D_n(q)\}_{n \in \mathbb{N}}$ be a sequence of skein elements in $\mathcal{S}(S^2)$. The evaluation of $D_n(q)$ gives in general a rational function. Using the observation in remark 3.2, one could study the tail of the sequence \mathcal{D} .

3.3 The Colored Kauffman Skein Relation

We start this section by proving the colored Kauffman skein relation in 4.5. This relation is implicit in the work of Yamada in [36]. The colored Kauffman skein relation will be used in the next section to understand the highest and the lowest coefficients of the colored Jones polynomial.

The following two Lemmas are basically due to Yamada [36]. We include the proof here with modification for completeness.

Lemma 3.3. *(The colored Kauffman skein relation) Let $n \geq 0$. Then we have*

$$\begin{array}{c} n+1 \quad n+1 \\ \diagdown \quad \diagup \\ \diagup \quad \diagdown \\ \diagup \quad \diagdown \end{array} = A^{2n+1} \left(\begin{array}{c} n+1 \quad n+1 \\ \text{arc } 1 \quad \text{arc } n \\ \text{arc } n \quad \text{arc } 1 \\ \text{arc } 1 \quad \text{arc } n \end{array} + A^{-(2n+1)} \begin{array}{c} n+1 \quad n+1 \\ \text{arc } n \quad \text{arc } 1 \\ \text{arc } 1 \quad \text{arc } n \\ \text{arc } n \quad \text{arc } 1 \end{array} \right)$$

Proof. Applying the Kauffman relation we obtain

$$\begin{array}{c} n+1 \quad n+1 \\ \diagdown \quad \diagup \\ \diagup \quad \diagdown \end{array} = A \left(\begin{array}{c} n+1 \quad n+1 \\ \text{crossing} \quad \text{crossing} \\ \text{crossing} \quad \text{crossing} \end{array} \right) + A^{-1} \left(\begin{array}{c} n+1 \quad n+1 \\ \text{crossing} \quad \text{crossing} \\ \text{crossing} \quad \text{crossing} \end{array} \right)$$

Using property (2) in 2.4 we obtain the result. \square

Note that if we specialize n to 1 in the previous Lemma we obtain the Kauffman skein relation. Recall that the quantum binomial coefficients are defined by:

$$\begin{bmatrix} n \\ k \end{bmatrix}_A = \frac{[n]!}{[k]![n-k]!}.$$

where $[n] = (-1)^{n-1} \Delta_{n-1}$ and $[n]! = [1] \dots [n]$.

Lemma 3.4. *Let $n \geq 0$. Then we have*

$$\begin{array}{c} \text{Diagram 1: Two lines crossing, each labeled } n. \end{array} = \sum_{k=0}^n C_{n,k} \begin{array}{c} \text{Diagram 2: A box with four horizontal segments labeled } n, n-k, n-k, n \text{ from top to bottom. Inside the box, two vertical arcs connect the top and bottom segments, each labeled } k. \end{array}$$

Where

$$C_{n,k} = A^{n(n-2k)} \begin{bmatrix} n \\ k \end{bmatrix}_A.$$

Proof. Lemma 4.5 implies that

$$\begin{array}{c} \text{Diagram 1: Two lines crossing, each labeled } n. \end{array} = \sum_{k=0}^n C'_{n,k} \begin{array}{c} \text{Diagram 2: A box with four horizontal segments labeled } n, n-k, n-k, n \text{ from top to bottom. Inside the box, two vertical arcs connect the top and bottom segments, each labeled } k. \end{array} \quad (3.1)$$

where $C'_{n,k}$ is a polynomial with integral coefficients in A . Let us prove by induction on n that we have

$$C'_{n,k} = C_{n,k}. \quad (3.2)$$

For $n = 1$ relation (3.2) holds since this is just the Kauffman skein relation.

Applying the identity (3.1) on each term of the colored Kauffman skein relation,

we obtain :

$$\begin{aligned}
\sum_{k=0}^n C'_{n,k} \text{ (diagram with } n \text{ top, } n-k \text{ left, } n \text{ right, } k \text{ top-right, } n-k \text{ bottom-right)} &= A^{2n-1} \sum_{k=0}^{n-1} C'_{n-1,k} \text{ (diagram with } n \text{ top, } n-k \text{ left, } n \text{ right, } k \text{ top-right, } n-k \text{ bottom-right)} \\
&+ A^{-2n+1} \sum_{k=0}^{n-1} C'_{n-1,k} \text{ (diagram with } n \text{ top, } n-k \text{ left, } n \text{ right, } k+1 \text{ top-right, } k+1 \text{ bottom-right)} \\
&= A^{2n-1} \sum_{k=0}^{n-1} C'_{n-1,k} \text{ (diagram with } n \text{ top, } n-k \text{ left, } n \text{ right, } k \text{ top-right, } n-k \text{ bottom-right)} \\
&+ A^{-2n+1} \sum_{k=1}^{n-1} C'_{n-1,k-1} \text{ (diagram with } n \text{ top, } n-k \text{ left, } n \text{ right, } k \text{ top-right, } k \text{ bottom-right)}
\end{aligned}$$

The skein elements $\text{(diagram with } n \text{ top, } n-k \text{ left, } n \text{ right, } k \text{ top-right, } n-k \text{ bottom-right)}$, where $0 \leq k \leq n$, are linearly independent (see remark 4.10) and hence

$$C'_{n,k} = A^{2n-1} C'_{n-1,k} + A^{-2n+1} C'_{n-1,k-1}. \quad (3.3)$$

However

$$\begin{aligned}
C_{n,k} &= A^{n(n-2k)} \left(A^{2k} \begin{bmatrix} n-1 \\ k \end{bmatrix}_A + A^{2k-2n} \begin{bmatrix} n-1 \\ k-1 \end{bmatrix}_A \right) \\
&= A^{n^2-2nk+2k} \begin{bmatrix} n-1 \\ k \end{bmatrix}_A + A^{n^2-2nk-2n+2k} \begin{bmatrix} n-1 \\ k-1 \end{bmatrix}_A
\end{aligned}$$

Hence

$$C_{n,k} = A^{2n-1} C_{n-1,k} + A^{-2n+1} C_{n-1,k-1}. \quad (3.4)$$

Relations (3.3) and (3.4) and the induction hypothesis yield the result. \square

Motivated by Lemma 4.5 we define *the n -colored states* for a link diagram D for every positive integer n . Suppose that the link diagram has k crossings. Label the

crossings of the link diagram D by $1, \dots, k$. An n -colored state $s^{(n)}$ for a link diagram D is a function $s^{(n)} : \{1, \dots, k\} \rightarrow \{-1, +1\}$. If the color n is clear from the context, we will drop n from the notation of a colored state.

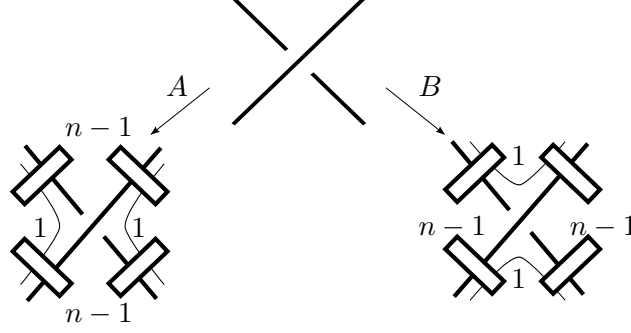


FIGURE 3.1. The n -colored A and B smoothings

Given a link diagram D and a colored state s for the diagram D . We construct a skein element $\Upsilon_D^{(n)}(s)$ obtained from D by replacing each crossing labeled $+1$ by an n -colored A -smoothing and each crossing labeled -1 by an n -colored B -smoothing, see Figure 3.1. Two particular skein elements obtained in this way are important to us. The skein element obtained by replacing each crossing by the n -colored A -smoothing will be called the n -colored A -state and denoted by $\Upsilon_D^{(n)}(s_+)$, where s_+ denotes the colored state for which $s_+(i) = +1$ for all i in $\{1, \dots, m\}$. The n -colored B -state is defined similarly. See Figure 3.2 for an example.

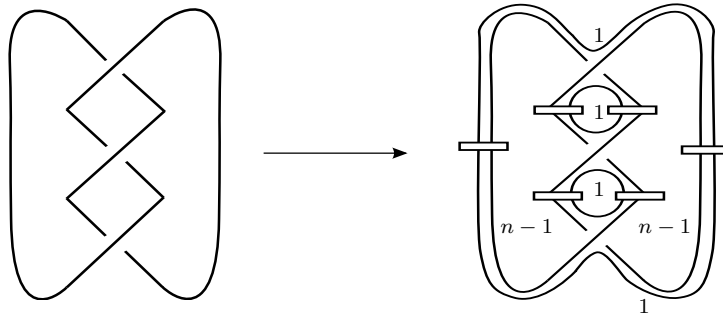


FIGURE 3.2. n -colored B -state

Consider a crossingless skein element D in $\mathcal{S}(S^2)$ consisting of arcs connecting Jones-Wenzl idempotents of various colors. Let \bar{D} be the diagram obtained from

D by replacing each idempotent $f^{(n)}$ with the identity id_n in TL_n . The diagram \bar{D} thus consists of non-intersecting circles. We say that D is adequate if each circle in \bar{D} passes at most once through any given region where we replaced the idempotents in D . See Figure 3.4 for a local picture of an adequate skein element and note that the circle indicated in the figure bounds a disk. Figure 3.3 shows an example of inadequate skein element on the left and an adequate skein element on the right.

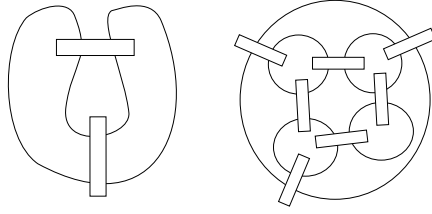


FIGURE 3.3. Adequate and inadequate skein elements. All arcs are colored n .

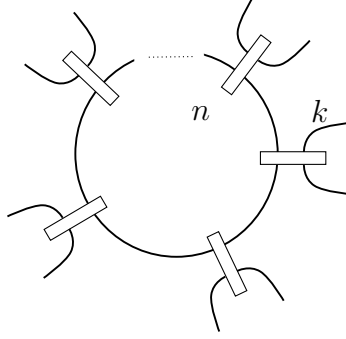


FIGURE 3.4. A local picture an adequate skein element

Using the convention in 3.2, we will denote by $m(f)$ to the minimum degree of f expressed as a Laurent series in q or in A . Furthermore, denote $D(S) := m(\bar{S})$. The following lemma is due to Armond [4].

Lemma 3.5. *If $S \in \mathcal{S}(S^2)$ is expressed as a single diagram containing the Jones-Wenzl idempotent, then $m(S) \geq D(S)$. If the diagram for S is an adequate skein diagram, then $m(S) = D(S)$.*

3.4 The Main Theorem

The colored Kauffman skein relation provides a natural framework to understand the highest and the lowest coefficients of the colored Jones polynomial. In this section we will use this relation to prove that the the highest (the lowest respectively) $4n$ coefficients of the n^{th} unreduced colored Jones polynomial agree up to a sign with the n -colored A -state (the n -colored B -state respectively). We use this result to prove existence of the the tail of the colored Jones polynomial.

Theorem 3.6. *Let L be an alternating link diagram. Then*

$$\tilde{J}_{n,L} \doteq_{4n} \Upsilon_L^{(n)}(s_-)$$

Proof. Assume that the link diagram L has k crossings and label the crossing of the link diagram by $1, \dots, k$. The colored Kauffman skein relation implies that

$$\tilde{J}_{n,L} \doteq \sum_s \alpha_L(n, s) \Upsilon_L^{(n)}(s)$$

where $\alpha_L(n, s) = A^{(2n-1)\sum_{i=1}^k s(i)}$ and the summation runs over all functions $s : \{1, 2, \dots, k\} \rightarrow \{-1, +1\}$. Now for any colored state s of the link diagram L there is a sequence of states s_0, s_1, \dots, s_r such that $s_0 = s_-$, $s_r = s$ and $s_{j-1}(i) = s_j(i)$ for all $i \in \{1, \dots, k\}$ except for one integer i_l for which $s_{j-1}(i_l) = -1$ and $s_j(i_l) = 1$. It is enough to show that the lowest $4n$ terms of $\alpha(n, s_-) \Upsilon_L^{(n)}(s_-)$ are never canceled by any term from $\alpha(n, s) \Upsilon_L^{(n)}(s)$ for any s . For any colored state s of the link diagram L one could write

$$\Upsilon_L^{(n)}(s) = \sum_{i_1, \dots, i_k=0}^{n-1} \prod_{j=1}^k C_{n-1, i_j} \Lambda_{s, (i_1, \dots, i_k)}$$

where $\Lambda_{s, (i_1, \dots, i_k)}$ is the skein element that we obtain by applying 4.8 to every crossing in $\Upsilon_L^{(n)}(s)$. The theorem follows from the following three lemmas.

□

Lemma 3.7.

$$m(\alpha_L(n, s_-)) = m(\alpha_L(n, s_1)) - 4n + 2$$

$$m(\alpha_L(n, s_r)) \leq m(\alpha_L(n, s_{r+1}))$$

$$m(C_{n-1, n-1}) - m(C_{n-1, n-2}) = -2$$

$$m(C_{n-1, i}) \leq m(C_{n-1, i-1}).$$

Proof. It is clear that

$$\alpha_L(n, s_-) = A^{k-2kn}$$

and

$$\alpha_L(n, s_1) = A^{-2+k+4n-2kn}$$

Furthermore,

$$\alpha_L(n, s_r) = A^{(2n-1)\sum_{i=1}^k s_r(i)} = A^{(2n-1)(-k+2r)} = A^{k-2kn-2r+4nr}$$

hence

$$m(\alpha_L(n, s_r)) - m(\alpha_L(n, s_{r+1})) = 2 - 4n.$$

Finally, it is clear that

$$m(C_{n, i}) = 2i^2 - 4in + n^2.$$

Hence, the result follows. □

Lemma 3.8.

$$m(\Lambda_{s_-, (n-1, \dots, n-1)}) = D(\Lambda_{s_1, (n-1, \dots, n-1)}) - 2.$$

$$D(\Lambda_{s, (i_1, \dots, i_{j-1}, i_j, i_{j+1}, \dots, i_k)}) = D(\Lambda_{s, (i_1, \dots, i_{j-1}, i_{j-1}, i_{j+1}, \dots, i_k)}) \pm 2.$$

Proof. When we replace the idempotent by the identity in the skein element $\Upsilon^{(n)}(s_-)$ we obtain the diagram $L^{n-1} \dot{\bigcup} C$ where C is a link diagram composed of a disjoint union of unit circles each one of them bounds a disk and L^{n-1} is the $(n-1)$ -parallel of L . Note that state $\overline{\Lambda_{s_-, (n-1, \dots, n-1)}}$ is exactly the all B -state of the link diagram L^n and it is also the all B -state of $L^{n-1} \dot{\bigcup} C$. Since L is alternating then the the number of circles in $\overline{\Lambda_{s_1, (n-1, \dots, n-1)}}$ is one less than the number of circles in $\overline{\Lambda_{s_-, (n-1, \dots, n-1)}}$. In other words, the number of circles in the all B -state of $\overline{\Upsilon^{(n)}(s_1)}$ is one less than the number of circles in the all B -state of the diagram $L^{n-1} \dot{\bigcup} C$. Thus,

$$D(\Lambda_{s_-, (n-1, \dots, n-1)}) = D(\Lambda_{s_1, (n-1, \dots, n-1)}) - 2.$$

Moreover the skein element $\Lambda_{s_-, (n-1, \dots, n-1)}$ is adequate since L is alternating. Hence by Lemma 3.5 we have

$$m(\Lambda_{s_-, (n-1, \dots, n-1)}) = D(\Lambda_{s_1, (n-1, \dots, n-1)}) - 2.$$

For the second part, note that the number of circles in the diagrams $\overline{\Lambda_{s, (i_1, \dots, i_{j-1}, i_j, i_{j+1}, \dots, i_k)}}$ and $\overline{\Lambda_{s, (i_1, \dots, i_{j-1}, i_j-1, i_{j+1}, \dots, i_k)}}$ differs by 1. Hence by 3.5 we obtain

$$D(\Lambda_{s, (i_1, \dots, i_{j-1}, i_j, i_{j+1}, \dots, i_k)}) = D(\Lambda_{s, (i_1, \dots, i_{j-1}, i_j-1, i_{j+1}, \dots, i_k)}) \pm 2$$

. □

Lemma 3.9.

$$m(\Upsilon^{(n)}(s_-)) = m((C_{n-1, n-1})^k \Lambda_{s_-, (n-1, \dots, n-1)}).$$

Proof. The previous two lemmas imply directly that the lowest term in $\Upsilon^{(n)}(s_-)$ is coming from the skein element $(C_{n-1, n-1})^k \Lambda_{s_-, (n-1, \dots, n-1)}$ and this term is never canceled by any other term in the summation. □

Theorem 3.10. *Let L be an alternating link diagram and let $\Upsilon^{(n+1)}(s_-)$ be its corresponding $(n+1)$ -colored B -state skein element. Then*

$$\Upsilon_L^{(n+1)}(s_-) \doteq_{4n} \tilde{J}_{n,L}$$

Proof. Since L is an alternating link diagram then the skein element $\Upsilon^{(n+1)}(s_-)$ must look locally as in Figure 3.5.

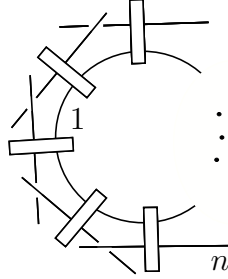
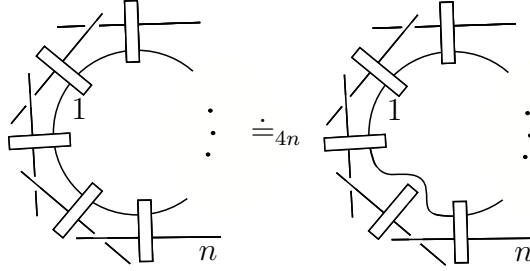


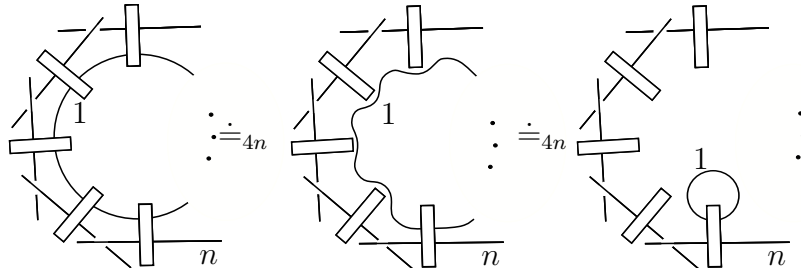
FIGURE 3.5. Local view of the skein element $\Upsilon^{(n+1)}(s_-)$

It follows from Theorem 9 and Lemma 10 in [4] that

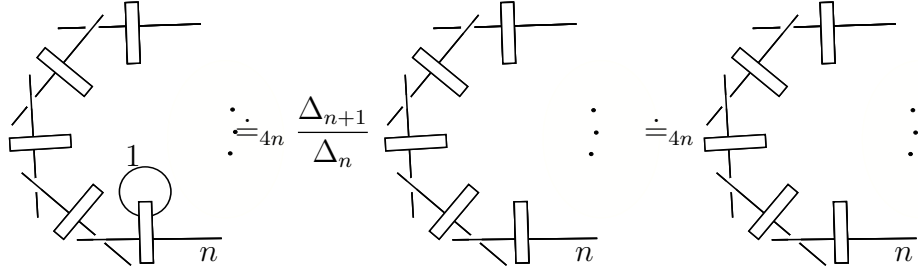


The details of the previous equation can be found in [4] and we will not repeat them here.

The previous step can be applied around the circle until we reach the final idempotent :



Equation 2.4 implies



Applying this procedure on every circle in $\Upsilon^{(n+1)}(s_-)$, we eventually obtain

$$\Upsilon^{(n+1)}(s_-) \doteq_{4n} \tilde{J}_{n,L}.$$

□

Theorems 5.6 and 5.7 imply immediately the following result.

Corollary 3.11. *Let L be an alternating link diagram. Then*

$$\tilde{J}_{n+1,L} \doteq_{4n} \tilde{J}_{n,L}$$

Chapter 4

The Bubble Skein Element and the Tail of the Knot 8_5

4.1 Introduction

Let L be an alternating link and let D be a reduced link diagram of L . Recall that $S_B(D)$ denotes the all- B smoothing state of D , the state obtained by replacing each crossing by a B smoothing. Let $S_B^{(n)}(D)$ be the skein element obtained from $S_B(D)$ by decorating each circle in this state with the n^{th} Jones-Wenzl idempotent and replacing each place where we had a crossing in D with the $(2n)^{th}$ projector. It was proven in [3] that for an adequate link L the first $4(n+1)$ coefficients of n^{th} unreduced colored Jones polynomial coincide with the first $4(n+1)$ coefficients of the skein element $S_B^{(n)}(D)$. Our work here initially aimed to understand $S_B^{(n)}(D)$ for an alternating link diagram D . Initial examinations of various examples of $S_B^{(n)}(D)$ showed that a certain skein element in the relative Kauffman bracket skein module of the disk with some marked points mostly shows up as sub-skein element of $S_B^{(n)}(D)$. We will call this skein element *the bubble skein element*. This chapter is based on our work in [11]. In this chapter we study a certain skein element in the relative Kauffman bracket skein module of the disk with some marked points, and expand this element in terms linearly independent elements of this module. Then we use this skein element in the study of the tail of 8_5 . The knot 8_5 is the first knot on the knot table that is not computable directly by the techniques developed [3]. In chapter 4 we use this skein element in various other applications.

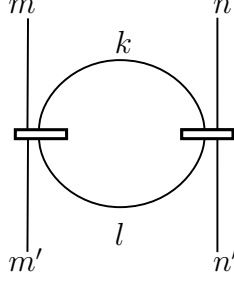


FIGURE 4.1. The bubble skein element $\mathcal{B}_{m',n'}^{m,n}(k,l)$

As we mentioned in earlier, we are interested in a particular skein element in the module $T_{m,n,n',m'}$. This element is shown in Figure 4.1 and it is denoted by $\mathcal{B}_{m',n'}^{m,n}(k,l)$, where $k, l \geq 1$. We will call such an element in $T_{m,n,n',m'}$ a *bubble skein element*. For every bubble skein element $\mathcal{B}_{m',n'}^{m,n}(k,l)$, the integers $m, n, m', n', k, l \geq 0$ and they satisfy $m + k = m' + l$ and $n + k = n' + l$. The main work of this chapter gives an expansion the bubble skein element $\mathcal{B}_{m',n'}^{m,n}(k,l)$, defined in the previous section, in terms of a set of $\mathbb{Q}(A)$ -linearly independent skein elements in the module $T_{m,n,n',m'}$ and gives an explicit determination of the coefficients obtained from this expansion.

Recall that the quantum binomial coefficients are defined by

$$\begin{bmatrix} l \\ i \end{bmatrix}_q = \frac{(q; q)_l}{(q; q)_i (q; q)_{l-i}}.$$

where $(a; q)_n$ is q -Pochhammer symbol which is defined as

$$(a; q)_n = \prod_{j=0}^{n-1} (1 - aq^j).$$

Remark 4.1. *Note that our choice for the quantum binomial coefficient is slightly different from the choice we made in the previous chapter. We will use the convention we have here in the consequent chapters as well.*

Theorem 4.2. (The bubble expansion formula) Let $m, n, m', n' \geq 0$, and $k \geq l$; $k, l \geq 1$. Then

$$\text{Diagram} = \sum_{i=0}^{\min(m, n, l)} \left[\begin{matrix} m & n \\ k & l \end{matrix} \right]_i \text{Diagram}$$

where

$$\left[\begin{matrix} m & n \\ k & l \end{matrix} \right]_i := (-A^2)^{i(i-l)} \frac{\prod_{j=0}^{l-i-1} \Delta_{k-j-1} \prod_{s=0}^{i-1} \Delta_{n-s-1} \Delta_{m-s-1}}{\prod_{t=0}^{l-1} \Delta_{n+k-t-1} \Delta_{m+k-t-1}} \left[\begin{matrix} l \\ i \end{matrix} \right]_{A^4} \prod_{j=0}^{l-i-1} \Delta_{m+n+k-i-j}.$$

We give two applications of the previous theorem. The first one gives a relation between the coefficient $\left[\begin{matrix} m & n \\ k & k \end{matrix} \right]_0$ and the theta graph $\Lambda(m, n, k)$ (see Figure 4.3) in $\mathcal{S}(S^2)$.

Proposition 4.3.

$$\text{Diagram} = \left[\begin{matrix} m & n \\ k & k \end{matrix} \right]_0 \Delta_{m+n}.$$

The second application that we give to the bubble expansion formula is showing that this expansion can be used to study and compute the tail of alternating links. In particular, we give a simple formula for the tail of the knot 8_5 :

Proposition 4.4.

$$T_{8_5}(q) = (q; q)_\infty^2 \sum_{k=0}^{\infty} \frac{q^{k+k^2}}{(q; q)_k} \left(\sum_{i=0}^k q^{(-2i(k-i))} \left[\begin{matrix} k \\ i \end{matrix} \right]_q^2 \right).$$

4.2 A Recursive Formula for the Bubble Skein Element

In this section we use the recursive definition of the Jones-Wenzl idempotent to obtain a recursive formula for the bubble skein element $\mathcal{B}_{m',n'}^{m,n}(k, l)$ in the module $T_{m,n,n',m'}$. To obtain a recursive formula for the element $\mathcal{B}_{m',n'}^{m,n}(k, l)$ we start by expanding the simple bubble element $\mathcal{B}_{m',n'}^{m,n}(k, 1)$ in Lemma 4.5 and then use this expansion to obtain a recursion equation for an arbitrary bubble skein element in Lemma 4.8. The recursive formula of $\mathcal{B}_{m',n'}^{m,n}(k, l)$ obtained in this section will be used in Theorem 4.11 to write a bubble skein element as a $\mathbb{Q}(A)$ -linear sum of linearly independent elements in $T_{m,n,n',m'}$.

We denote the rational functions $\frac{\Delta_{n+k}\Delta_{m+k-1}-\Delta_n\Delta_{m-1}}{\Delta_{n+k-1}\Delta_{m+k-1}}$ and $\frac{\Delta_{m-1}\Delta_{n-1}}{\Delta_{n+k-1}\Delta_{m+k-1}}$ by $\alpha_{m,n}^k$ and $\beta_{m,n}^k$, respectively.

Lemma 4.5. *Let $m, n, m', n' \geq 0$; $k \geq 1$. Then we have*

$$\text{Bubble}(m, n, m', n', k, 1) = \alpha_{m,n}^k \text{Bubble}(m, n, m', n', k-1, 1) + \beta_{m,n}^k \text{Bubble}(m, n, m', n', 1, k).$$

Proof. First we consider the trivial cases when one of the integers m, n, m', n' is zero. Observe that $m + k = 1 + m'$ and $n + k = 1 + n'$. Since $k \geq 1$, we know that $m \leq m'$ and $n \leq n'$. If $m' = n' = 0$, then this implies that m and n must be zero and k is 1. Hence $\mathcal{B}_{0,0}^{0,0}(1, 1) = \alpha_{0,0}^1 = \Delta_1$ and we are done. Here we used our convention that a diagram is zero if it has a strand colored by a negative number. If $\min(m, n) = 0$ or $\min(m', n') = 0$, then the result follows from (2.4).

When $\min(m, n) \neq 0$, we use induction on k . For $k = 1$ we apply the recursive definition of the Jones-Wenzel idempotent (2.1) on the projector $f^{(m+1)}$ that

appears in $\mathcal{B}_{m',n'}^{m,n}(1,1)$ to obtain

$$\begin{array}{c} m \\ | \\ \text{---} \\ | \\ m' \end{array} \begin{array}{c} 1 \\ \bigcirc \\ 1 \end{array} \begin{array}{c} n \\ | \\ \text{---} \\ | \\ n' \end{array} = \begin{array}{c} m \\ | \\ \text{---} \\ | \\ m' \end{array} \begin{array}{c} 1 \\ \bigcirc \\ 1 \end{array} \begin{array}{c} n \\ | \\ \text{---} \\ | \\ n' \end{array} - \frac{\Delta_{m-1}}{\Delta_m} \begin{array}{c} m \\ | \\ \text{---} \\ | \\ m' \end{array} \begin{array}{c} 1 \\ \text{---} \\ 1 \end{array} \begin{array}{c} n \\ | \\ \text{---} \\ | \\ n' \end{array}. \quad (4.1)$$

Using identity (2.4) in the first term and expanding the projector $f^{(n+1)}$ the second term in (5.11) implies

$$\begin{array}{c} m \\ | \\ \text{---} \\ | \\ m' \end{array} \begin{array}{c} 1 \\ \bigcirc \\ 1 \end{array} \begin{array}{c} n \\ | \\ \text{---} \\ | \\ n' \end{array} = \frac{\Delta_{n+1}\Delta_m - \Delta_n\Delta_{m-1}}{\Delta_n\Delta_m} \begin{array}{c} m \\ | \\ \text{---} \\ | \\ m' \end{array} + \frac{\Delta_{m-1}\Delta_{n-1}}{\Delta_n\Delta_m} \begin{array}{c} m \\ | \\ \text{---} \\ | \\ m' \end{array} \begin{array}{c} 1 \\ \text{---} \\ 1 \end{array} \begin{array}{c} n \\ | \\ \text{---} \\ | \\ n' \end{array}. \quad (4.2)$$

For $k \geq 2$, we use the recursive definition (2.1) on the projector $f^{(m+k)}$ that appears in $\mathcal{B}_{m',n'}^{m,n}(k,1)$. Hence

$$\begin{array}{c} m \\ | \\ \text{---} \\ | \\ m' \end{array} \begin{array}{c} k \\ \bigcirc \\ 1 \end{array} \begin{array}{c} n \\ | \\ \text{---} \\ | \\ n' \end{array} = \begin{array}{c} m \\ | \\ \text{---} \\ | \\ m' \end{array} \begin{array}{c} k-1 \\ \bigcirc \\ 1 \end{array} \begin{array}{c} n \\ | \\ \text{---} \\ | \\ n' \end{array} - \frac{\Delta_{m+k-2}}{\Delta_{m+k-1}} \begin{array}{c} m \\ | \\ \text{---} \\ | \\ m' \end{array} \begin{array}{c} k-1 \\ \text{---} \\ 1 \end{array} \begin{array}{c} n \\ | \\ \text{---} \\ | \\ n' \end{array}. \quad (4.3)$$

Using identity (2.4) and expanding the projector $f^{(n+k)}$ in (4.3) implies

$$\begin{array}{c} m \\ | \\ \text{---} \\ | \\ m' \end{array} \begin{array}{c} k \\ \bigcirc \\ 1 \end{array} \begin{array}{c} n \\ | \\ \text{---} \\ | \\ n' \end{array} = \frac{\Delta_{n+k}\Delta_{m+k-1} - \Delta_{n+k-1}\Delta_{m+k-2}}{\Delta_{m+k-1}\Delta_{n+k-1}} \begin{array}{c} m \\ | \\ \text{---} \\ | \\ m' \end{array} \begin{array}{c} k-1 \\ \text{---} \\ 1 \end{array} \begin{array}{c} n \\ | \\ \text{---} \\ | \\ n' \end{array} + \frac{\Delta_{m+k-2}\Delta_{n+k-2}}{\Delta_{m+k-1}\Delta_{n+k-1}} \begin{array}{c} m \\ | \\ \text{---} \\ | \\ m' \end{array} \begin{array}{c} k-1 \\ \bigcirc \\ 1 \end{array} \begin{array}{c} n \\ | \\ \text{---} \\ | \\ n' \end{array}. \quad (4.4)$$

We apply the induction hypothesis on the bubble skein element $\mathcal{B}_{m',n'}^{m,n}(k-1,1)$ that appears in the second term of the last equation:

$$\begin{aligned}
\text{Diagram 1} &= \frac{\Delta_{n+k}\Delta_{m+k-1} - \Delta_{n+k-1}\Delta_{m+k-2}}{\Delta_{m+k-1}\Delta_{n+k-1}} \text{Diagram 2} \\
&+ \frac{\Delta_{m+k-2}\Delta_{n+k-2}}{\Delta_{m+k-1}\Delta_{n+k-1}} \left(\frac{\Delta_{n+k-1}\Delta_{m+k-2} - \Delta_n\Delta_{m-1}}{\Delta_{m+k-2}\Delta_{n+k-2}} \text{Diagram 3} \right) \\
&+ \frac{\Delta_{m-1}\Delta_{n-1}}{\Delta_{m+k-2}\Delta_{n+k-2}} \text{Diagram 4}.
\end{aligned}$$

Collecting similar terms together, we obtain

$$\begin{aligned}
& \text{Diagram 1} = \frac{\Delta_{n+k} \Delta_{m+k-1} - \Delta_n \Delta_{m-1}}{\Delta_{n+k-1} \Delta_{m+k-1}} \text{Diagram 2} \\
& + \frac{\Delta_{m-1} \Delta_{n-1}}{\Delta_{n+k-1} \Delta_{m+k-1}} \text{Diagram 3} .
\end{aligned}$$

Remark 4.6. *Note that, while the symmetry with respect to the variables m and n in the function $\beta_{m,n}^k$ is clear, the rational function $\alpha_{m,n}^k$ appears to be asymmetric*

Now suppose that $\min(m, n) \neq 0$ and apply the recursive definition of the Jones-Wenzel idempotent on the projector $f^{(m+k)}$ that appears in $\mathcal{B}_{m', n'}^{m, n}(k, l)$

$$\begin{array}{c} m \\ | \\ \text{---} \\ | \\ m' \end{array} \begin{array}{c} n \\ | \\ \text{---} \\ | \\ n' \end{array} \begin{array}{c} k \\ \text{---} \\ l \end{array} = \begin{array}{c} m \\ | \\ \text{---} \\ | \\ m' \end{array} \begin{array}{c} n \\ | \\ \text{---} \\ | \\ n' \end{array} \begin{array}{c} k-1 \\ \text{---} \\ l-1 \end{array} - \frac{\Delta_{m+k-2}}{\Delta_{m+k-1}} \begin{array}{c} m \\ | \\ \text{---} \\ | \\ m' \end{array} \begin{array}{c} n \\ | \\ \text{---} \\ | \\ n' \end{array} \begin{array}{c} k-1 \\ \text{---} \\ l-1 \end{array} \quad (4.6)$$

Removing the loop that appears in the first term and expanding the projector $f^{(n+k)}$ in the second term of (4.6) we obtain

$$\begin{array}{c} m \\ | \\ \text{---} k \text{---} \\ | \\ n' \\ m' \end{array} = \frac{\Delta_{n+k}\Delta_{m+k-1}-\Delta_{n+k-1}\Delta_{m+k-2}}{\Delta_{n+k-1}\Delta_{m+k-1}} \begin{array}{c} m \\ | \\ \text{---} k-1 \text{---} \\ | \\ n' \\ m' \end{array} + \frac{\Delta_{m+k-2}\Delta_{n+k-2}}{\Delta_{n+k-1}\Delta_{m+k-1}} \cdot \begin{array}{c} m \\ | \\ \text{---} k-1 \text{---} \\ | \\ n' \\ m' \end{array}. \quad (4.7)$$

If $l = 1$ then the result follows from Lemma 4.5. Otherwise we apply Lemma 4.5 to the skein element $\mathcal{B}_{m',n'}^{m,n}(k-1,1)$ appearing in the second term of (4.7) to obtain

$$\begin{aligned}
& \text{Diagram 1} = \frac{\Delta_{n+k} \Delta_{m+k-1} - \Delta_{n+k-1} \Delta_{m+k-2}}{\Delta_{n+k-1} \Delta_{m+k-1}} \text{Diagram 2} \\
& + \frac{\Delta_{m+k-2} \Delta_{n+k-2}}{\Delta_{n+k-1} \Delta_{m+k-1}} \left(\frac{\Delta_{n+k-1} \Delta_{m+k-2} - \Delta_n \Delta_{m-1}}{\Delta_{n+k-2} \Delta_{m+k-2}} \text{Diagram 3} \right) \\
& + \frac{\Delta_{m-1} \Delta_{n-1}}{\Delta_{n+k-2} \Delta_{m+k-2}} \text{Diagram 4}
\end{aligned}$$

The last equation implies:

$$\begin{aligned}
& \text{Diagram 1} = \frac{\Delta_{n+k} \Delta_{m+k-1} - \Delta_n \Delta_{m-1}}{\Delta_{n+k-1} \Delta_{m+k-1}} \text{Diagram 2} + \frac{\Delta_{m-1} \Delta_{n-1}}{\Delta_{n+k-1} \Delta_{m+k-1}} \text{Diagram 3} . \\
& \square
\end{aligned}$$

Remark 4.9. *Let $m, n, m', n' \geq 0$. Without loss of generality assume that $m+n' \geq n+m'$. In the space in $T_{m,n,n',m'}$, there is a one-to-one correspondence between the two set of element shown in Figure 4.2. The correspondence is shown also in the same Figure and it can be parameterized by an integer i . Note that the diagonal line in the Figure represents $\frac{1}{2}(m+n'-n-m')$ parallel lines. The skein elements on the right-hand side of Figure 4.2 form a basis for the space $T_{m,n,n',m'}$. For a proof of this fact see Lemma 14.9 in [22]. On the other hand the skein elements of the left-hand side spans the space $T_{m,n,n',m'}$. See also the proof of Lemma 14.9 in [22]. One concludes that, by the correspondence shown in Figure 4.2 the skein elements on the left-hand side of Figure 4.2 must be linearly independent and hence they form a basis for the space $T_{m,n,n',m'}$.*

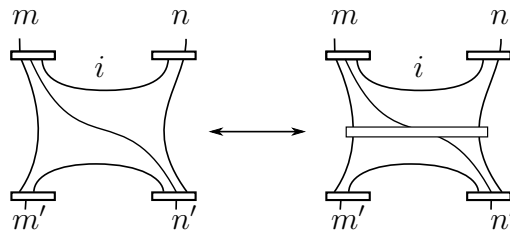


FIGURE 4.2. Correspondence between two bases in the module $T_{m,n,n',m'}$.

Remark 4.10. *We are interested in the coefficients the bubble skein element $\mathcal{B}_{m',n'}^{m,n}(k,l)$ in terms of the basis shown on the left-hand side in Figure 4.2. Since $m+k = m'+l$ and $n+k = n'+l$ then we must have $m+n' = n+m'$ and hence the*

diagonal line in the basis shown on the left-hand side in Figure 4.2 will not appear when we expand the element $\mathcal{B}_{m',n'}^{m,n}(k,l)$ in terms of this basis.

4.3 The Bubble Expansion Formula

In this section we will use the recursive formula we obtained in Lemma 4.8 for $\mathcal{B}_{m',n'}^{m,n}(k,l)$ to expand this element as a $\mathbb{Q}(A)$ -linear sum of certain linearly independent skein elements in $T_{m,n,n',m'}$. Then we will use Theorem 4.11 together with Lemma 4.8 to determine a recursive formula for the coefficients of $\mathcal{B}_{m',n'}^{m,n}(k,l)$ in terms of these linearly independent elements. Finally, the recursive formula will be used to determine a closed form of these coefficients.

Theorem 4.11. *Let $m, n, m', n' \geq 0$; $k, l \geq 1$. Then*

(1) For $k \geq l$:

$$\begin{array}{c} m \\ | \\ \text{---} \\ | \\ m' \end{array} \quad \begin{array}{c} k \\ \bigcirc \\ l \end{array} \quad \begin{array}{c} n \\ | \\ \text{---} \\ | \\ n' \end{array} = \sum_{i=0}^{\min(m,n,l)} \left[\begin{array}{cc} m & n \\ k & l \end{array} \right]_i \quad \begin{array}{c} m \\ | \\ \text{---} \\ | \\ m' \end{array} \quad \begin{array}{c} i \\ \bigcap \\ k-l+i \\ \bigcup \\ n \\ | \\ \text{---} \\ | \\ n' \end{array} . \quad (4.8)$$

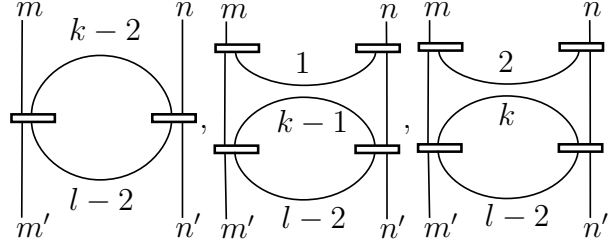
(2) For $l \geq k$:

$$\begin{array}{c} m \\ | \\ \text{---} \\ | \\ m' \end{array} \begin{array}{c} \text{---} \\ | \\ n \\ | \\ n' \end{array} \begin{array}{c} k \\ \text{---} \\ l \end{array} = \sum_{i=0}^{\min(m', n', k)} \left[\begin{array}{cc} n' & m' \\ k & l \end{array} \right]_i \begin{array}{c} m \\ \text{---} \\ | \\ \text{---} \\ | \\ m' \end{array} \begin{array}{c} n \\ \text{---} \\ | \\ \text{---} \\ | \\ n' \end{array} \begin{array}{c} l-k+i \\ \text{---} \\ i \end{array}. \quad (4.9)$$

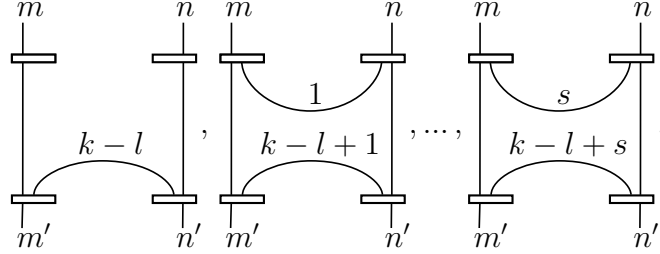
where $\begin{bmatrix} m & n \\ k & l \end{bmatrix}_i := \begin{bmatrix} m & n \\ k & l \end{bmatrix}_i (A)$ and $\begin{bmatrix} n' & m' \\ k & l \end{bmatrix}_i := \begin{bmatrix} n' & m' \\ k & l \end{bmatrix}_i (A)$ are rational functions.

Proof. (1) The trivial cases when $\min(m, n, l) \leq 1$ were discussed in Lemma 4.8. Suppose that $\min(m, n, l) \geq 2$ and consider the identity (4.5). We apply this identity to the bubble skein elements appearing in the first and the second terms of

(4.5). We obtain that $\mathcal{B}_{m',n'}^{m,n}(k,l)$ is equal to a $\mathbb{Q}(A)$ -linear sum of the three skein elements



Note that a bubble skein element appears in each of the three elements above. Moreover, each bubble has an index on at least one of its strands that is less than the index of the corresponding strand in (4.5). One could apply the identity (4.5) iteratively on each bubble that appears in the sum. This iterative process will eventually terminate all bubbles in each element in the summation. This yields that $\mathcal{B}_{m',n'}^{m,n}(k,l)$ is equal to a $\mathbb{Q}(A)$ -linear sum of the $T_{m,n,n',m'}$ skein elements



where $s = \min(m, n, l)$. Now the result follows by noticing that the variables m, n, m', n', k and l are related by the equations $m + k = m' + l$ and $n + k = n' + l$ and hence it is sufficient to index the coefficients in the expansion of $\mathcal{B}_{m',n'}^{m,n}(k,l)$ in terms of the previous skein elements by five indices. (2) Follows from (1). \square

Now we determine the coefficients $\begin{bmatrix} m & n \\ k & l \end{bmatrix}_i$.

Proposition 4.12. *Let $m, n, m', n' \geq 0$, $k, l \geq 1$. Let $\mathcal{B}_{m',n'}^{m,n}(k,l)$ be a bubble skein element in $T_{m,n,n',m'}$ such that $k \geq l$. Then, for $0 \leq i \leq \min(m, n, l)$, the rational*

function $\begin{bmatrix} m & n \\ k & l \end{bmatrix}_i$ satisfies the following recursive identity:

$$\left[\begin{array}{cc} m & n \\ k & l \end{array} \right]_i = \alpha_{m,n}^k \times \left[\begin{array}{cc} m & n \\ k-1 & l-1 \end{array} \right]_i + \beta_{m,n}^k \times \left[\begin{array}{cc} m-1 & n-1 \\ k & l-1 \end{array} \right]_{i-1}. \quad (4.10)$$

Proof. Substitute (4.8) in both sides of (4.5):

$$\begin{aligned} \sum_{i=0}^{\min(m,n,l)} \left[\begin{array}{cc} m & n \\ k & l \end{array} \right]_i & \times \text{Diagram 1} = \alpha_{m,n}^k \sum_{i=0}^{\min(m,n,l-1)} \left[\begin{array}{cc} m & n \\ k-1 & l-1 \end{array} \right]_i \times \text{Diagram 2} \\ & + \beta_{m,n}^k \sum_{i=0}^{\min(m-1,n-1,l-1)} \left[\begin{array}{cc} m-1 & n-1 \\ k & l-1 \end{array} \right]_i \times \text{Diagram 3}. \end{aligned}$$

Diagram 1: A vertical line with top nodes m and n , and bottom nodes m' and n' . A horizontal bar is at the top. A curved line connects the two vertical lines at height i from the bottom, labeled i above and $k-l+i$ below. Another curved line connects them at height $k-l+i$ from the bottom, labeled $k-l+i$ below.

Diagram 2: Similar to Diagram 1, but the bottom curved line is labeled $k-l+i$ below.

Diagram 3: Similar to Diagram 1, but the top nodes are $m-1$ and $n-1$, and the bottom curved line is labeled $k-l+i+1$ below. There is an additional curved line at the top labeled 1 above and i below.

Hence

$$\begin{aligned} \sum_{i=0}^{\min(m,n,l)} \left[\begin{array}{cc} m & n \\ k & l \end{array} \right]_i & \times \text{Diagram 1} = \sum_{i=0}^{\min(m,n,l-1)} \alpha_{m,n}^k \times \left[\begin{array}{cc} m & n \\ k-1 & l-1 \end{array} \right]_i \times \text{Diagram 2} \\ & + \sum_{i=0}^{\min(m-1,n-1,l-1)} \beta_{m,n}^k \times \left[\begin{array}{cc} m-1 & n-1 \\ k & l-1 \end{array} \right]_i \times \text{Diagram 3}. \end{aligned}$$

Diagram 1: Same as in the previous block.

Diagram 2: Same as in the previous block.

Diagram 3: Similar to Diagram 1, but the top nodes are $m-1$ and $n-1$, and the bottom curved line is labeled $k-l+i+1$ below. There is an additional curved line at the top labeled $i+1$ above and i below.

The latter can be written as

$$\begin{aligned}
\sum_{i=0}^{\min(m,n,l)} \left[\begin{array}{cc} m & n \\ k & l \end{array} \right]_i &= \sum_{i=0}^{\min(m,n,l-1)} \alpha_{m,n}^k \times \left[\begin{array}{cc} m & n \\ k-1 & l-1 \end{array} \right]_i \\
&+ \sum_{i=1}^{\min(m,n,l)} \beta_{m,n}^k \times \left[\begin{array}{cc} m-1 & n-1 \\ k & l-1 \end{array} \right]_{i-1}
\end{aligned}$$

Now note that the elements $\left[\begin{array}{cc} m & n \\ k & l \end{array} \right]_i$, where $0 \leq i \leq \min(m, n, l)$, are linearly independent in the module $T_{m,n,n',m'}$ by Remarks 4.9 and 4.10. Hence we conclude that

$$\left[\begin{array}{cc} m & n \\ k & l \end{array} \right]_i = \alpha_{m,n}^k \times \left[\begin{array}{cc} m & n \\ k-1 & l-1 \end{array} \right]_i + \beta_{m,n}^k \times \left[\begin{array}{cc} m-1 & n-1 \\ k & l-1 \end{array} \right]_{i-1}.$$

□

Remark 4.13. The coefficients $\left[\begin{array}{cc} m & n \\ k & l \end{array} \right]_i$ behave like the binomial coefficients $\binom{l}{i}$

in the sense that $\left[\begin{array}{cc} m & n \\ k & l \end{array} \right]_i = 0$ when $i < 0$ or $i > l$. Note also that the recursion formula for $\left[\begin{array}{cc} m & n \\ k & l \end{array} \right]_i$, when one focuses the variables l and i , is analogous to the recursion formula of the binomial coefficients $\binom{l}{i}$.

The following theorem gives a closed formula for the rational function $\left[\begin{array}{cc} m & n \\ k & l \end{array} \right]_i$.

Theorem 4.14. *Let $m, n, k, l \geq 0$, and $k \geq l$ and $0 \leq i \leq \min(m, n, l)$. Then*

$$\left[\begin{array}{cc} m & n \\ k & l \end{array} \right]_i = (-A^2)^{i(i-l)} \frac{\prod_{j=0}^{l-i-1} \Delta_{k-j-1} \prod_{s=0}^{i-1} \Delta_{n-s-1} \Delta_{m-s-1}}{\prod_{t=0}^{l-1} \Delta_{n+k-t-1} \Delta_{m+k-t-1}} \left[\begin{array}{c} l \\ i \end{array} \right]_{A^4} \prod_{j=0}^{l-i-1} \Delta_{m+n+k-i-j}. \quad (4.11)$$

Proof. This equation agrees with the recursion identity (4.10). \square

The symmetry of the bubble skein element, or the previous formula for the coefficients $\left[\begin{array}{cc} m & n \\ k & l \end{array} \right]_i$, implies immediately the following.

Proposition 4.15. *Let $m, n, k, l \geq 0$. Let $k \geq l$. Then*

$$\left[\begin{array}{cc} m & n \\ k & l \end{array} \right]_i = \left[\begin{array}{cc} n & m \\ k & l \end{array} \right]_i. \quad (4.12)$$

It is preferred sometimes to write the the coefficients $\left[\begin{array}{cc} m & n \\ k & l \end{array} \right]_i$ in terms of quantum integers rather than deltas. Recall that $\Delta_n = (-1)^n [n+1]$ and hence the sign of the term $\prod_{j=0}^{l-i-1} [k-j]$ can be easily calculated to be $(-1)^{-(\frac{1}{2})(i-l)(-1+i+2k-l)}$. Similarly, the sign of $\prod_{s=0}^{i-1} [n-s]$ is $(-1)^{-(\frac{1}{2})i(1+i-2n)}$, the sign of $\prod_{t=0}^{l-1} [n+k-t]$ is $(-1)^{-(\frac{1}{2})l(1-2k+l-2n)}$, and the sign of $\prod_{j=0}^{l-i-1} [m+n+k-i-j+1]$ is $(-1)^{-(\frac{1}{2})(i-l)(1+i+2k-l+2m+2n)}$. Thus the exponent of -1 of the whole term is $-i-2ik-l+2il+4kl-2l^2+2lm+2ln = i+l \pmod{2}$. Hence the previous theorem can be rewritten as follows:

Corollary 4.16. *Let $m, n, k, l \geq 0$. Let $k \geq l$ and $0 \leq i \leq \min(m, n, l)$. Then*

$$\left[\begin{array}{cc} m & n \\ k & l \end{array} \right]_i = (-1)^{i+l} a^{i(i-l)} \frac{\prod_{j=0}^{l-i-1} [k-j] \prod_{s=0}^{i-1} [n-s][m-s]}{\prod_{t=0}^{l-1} [n+k-t][m+k-t]} \left[\begin{array}{c} l \\ i \end{array} \right]_{a^2} \prod_{j=0}^{l-i-1} [m+n+k-i-j+1].$$

4.4 Applications

In this section we relate the coefficient $\left[\begin{array}{cc} m & n \\ k & k \end{array} \right]_0$ to the theta graph evaluation in S^2 and use the bubble formula to compute the tail of the knot 8_5 .

4.4.1 The Theta Graph

A theta graph is a spin network in S^2 that plays an important role in computing arbitrary spin network in S^2 . The evaluation of a theta graph in $\mathcal{S}(S^2)$ is equivalent to find the evaluation of the skein element in Figure 4.3. Explicit determination

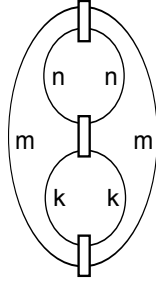


FIGURE 4.3. The skein element $\Lambda(m, n, k)$

of this skein element is done in [19] and [25]. We will denote this skein element by $\Lambda(m, n, k)$. Our first immediate application of the bubble expansion formula is computing this skein element. The following lemma shows that $\left[\begin{array}{cc} m & n \\ k & k \end{array} \right]_0$ is almost equal to the evaluation of this skein element.

Lemma 4.17.

$$\begin{array}{c} \text{Diagram: A large oval with two internal circles. The top circle has two nodes labeled 'n' and the bottom circle has two nodes labeled 'k'. The left and right arcs of the large oval are labeled 'm'. There are four small vertical rectangles at the top, bottom, and on the left and right arcs of the internal circles. \end{array} = \begin{bmatrix} m & n \\ k & k \end{bmatrix}_0 \Delta_{m+n}. \quad (4.13)$$

Proof. We apply the bubble skein formula (4.8) on that bubble $\mathcal{B}_{m,n}^{m,n}(k,k)$ appears in Figure 4.3:

$$\begin{array}{c} \text{Diagram: Same as in Lemma 4.17. \end{array} = \sum_{i=0}^{\min(m,n,k)} \begin{bmatrix} m & n \\ k & k \end{bmatrix}_i \begin{array}{c} \text{Diagram: A large oval with two internal circles. The top circle has two nodes labeled 'n' and the bottom circle has two nodes labeled 'i'. The left and right arcs of the large oval are labeled 'm'. The top arc of the bottom circle is labeled 'n-i' and the bottom arc is labeled 'm-i'. There are four small vertical rectangles at the top, bottom, and on the left and right arcs of the internal circles. \end{array}$$

The previous summation is zero except when $i = 0$ and hence it reduces to

$$\begin{bmatrix} m & n \\ k & k \end{bmatrix}_0 \begin{array}{c} \text{Diagram: Same as in Lemma 4.17. \end{array} = \begin{bmatrix} m & n \\ k & k \end{bmatrix}_0 \Delta_{m+n}.$$

□

Remark 4.18. In the previous lemma one could apply the bubble skein formula on the other bubbles in the skein element 4.3 and obtain

$$\begin{array}{c} \text{Diagram: Same as in Lemma 4.17. \end{array} = \begin{bmatrix} m & n \\ k & k \end{bmatrix}_0 \Delta_{m+n} = \begin{bmatrix} m & k \\ n & n \end{bmatrix}_0 \Delta_{m+k} = \begin{bmatrix} n & k \\ m & m \end{bmatrix}_0 \Delta_{n+k}.$$

This reflects the symmetry of the theta graph.

4.4.2 The Head and the Tail of Alternating Knots

We recall here some basic facts about the tail of the colored Jones polynomial. Recall that $B(D)$ denotes the B -graph associated with the state $S_B(D)$. The *reduced B -graph* of D , denoted by $B'(D)$, is defined to be the graph that is obtained from $B'(D)$ by keeping the same set of vertices of $B(D)$ and replacing parallel edges by a single edge. See for 5.5 an example. We define the A - graph similarly.

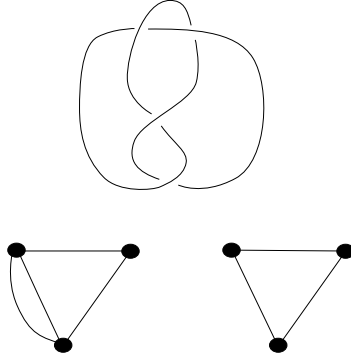


FIGURE 4.4. The knot 4_1 , its A -graph (left). Its reduced A -graph (right)

Let D be a link diagram and consider the skein element obtained from $S_B(D)$ by decorating each circle in $S_B(D)$ with the n^{th} Jones-Wenzl idempotent and replacing each dashed line in $S_B(D)$ with the $(2n)^{th}$ Jones-Wenzl idempotent. See Figure 4.5 for an example. Write $S_B^{(n)}(D)$ to denote this skein element.

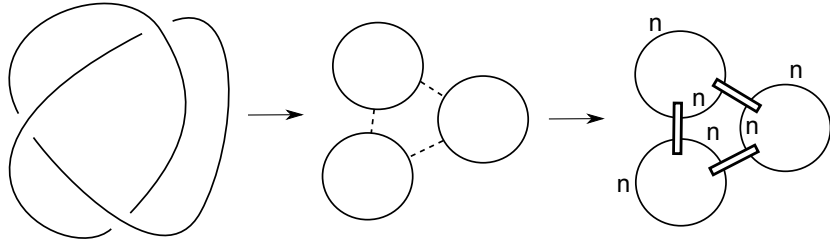


FIGURE 4.5. Obtaining $S_B^{(n)}(D)$ from a knot diagram D

We will need the following theorem.

Theorem 4.19. (*C. Armond [4]*) *Let L be a link in S^3 and D be a reduced alternating knot diagram of L . Then*

$$\tilde{J}_{n,L}(A) \doteq_{4(n+1)} S_B^{(n)}(D).$$

Theorem 4.19 has an important consequence, which basically tells us that the tail (the head) of an alternating link only depends on the reduced A -graph (reduced B -graph):

Theorem 4.20. (*C. Armond, O. Dasbach [3]*) *Let L_1 and L_2 be two alternating links with alternating diagrams D_1 and D_2 . If the graph $A'(D_1)$ coincides with $A'(D_2)$, then $T_{K_1} = T_{K_2}$. Similarly, if $B'(D_1)$ coincides with $B'(D_2)$, then $H_{K_1} = H_{K_2}$.*

Finding an exact form for the head and tail series is an interesting task. Explicit calculations were done on the knot table to determine these two power series in [3]. Using multiple techniques Armond and Dasbach determined the head and tail for an infinite family of knots and links. The knot 8_5 , Figure 4.6, is the first knot on the knot table whose tail could not be determined by a direct application of techniques in [3].

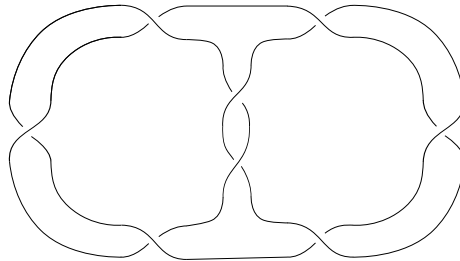


FIGURE 4.6. The knot 8_5

The techniques we developed here appear to be helpful in understanding the head and the tail for some knots. We demonstrate this by studying the family of knots in Figure 4.7. Note that we obtain the knot 8_5 from this family by replacing each crossing region by a single crossing.

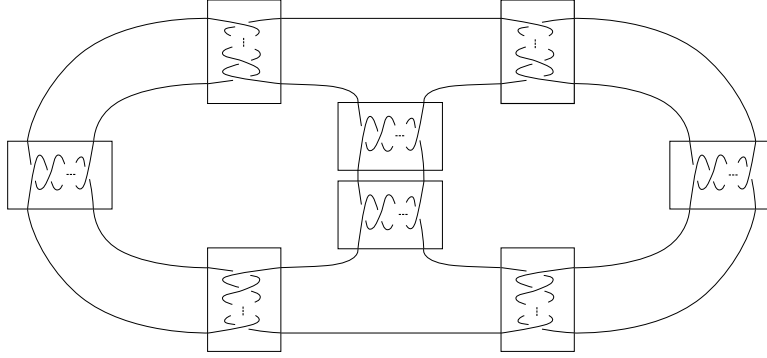


FIGURE 4.7. The knot Γ

The reduced B -graph for each knot in this family can be easily seen to coincide with the graph in Figure 5.4.



FIGURE 4.8. The reduced B -graph for Γ

Hence the skein element $S_B^{(n)}$ for any knot from the family of the knots shown in 4.7 is given in Figure 4.9. Note that the bubble skein element appears in multiple places in this skein element.

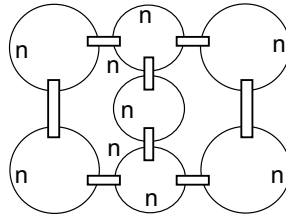


FIGURE 4.9. The skein element $S_B^{(n)}(\Gamma)$

Let Γ be any knot from the family in Figure 4.7. Theorem 4.19 implies

$$\tilde{J}_{n,\Gamma}(A) \doteq_{4(n+1)} \begin{array}{c} \text{Diagram of a skein element } \tilde{J}_{n,\Gamma}(A) \text{ consisting of six circles arranged in a 2x3 grid. Each circle is labeled } n. \text{ The circles are connected by horizontal and vertical lines, with some lines having small bars.} \end{array}.$$

Remark 4.21. *The algorithm of Masbaum and Vogel in [25] can be used to compute the evaluation of any quantum spin network in $\mathcal{S}(S^2)$. In particular, it can be used to give a formula for the skein element $S_B^{(n)}(\Gamma)$. However, it is difficult to compute the tail of Γ using the formula obtained from this algorithm. For this reason, we will use the techniques we developed here to compute the evaluation of the skein element $S_B^{(n)}(\Gamma)$.*

Now we compute the tail of the knot Γ .

Lemma 4.22.

$$\tilde{J}_{n,\Gamma}(A) \doteq_{4(n+1)} \sum_{i=0}^n \sum_{j=0}^n \begin{bmatrix} n & n \\ n & n \end{bmatrix}_i \begin{bmatrix} n & n \\ n & n \end{bmatrix}_j \begin{bmatrix} i & n \\ n & n-j \end{bmatrix}_0 \begin{bmatrix} j & n \\ n & n-i \end{bmatrix}_0 \begin{bmatrix} j & i \\ n & n \end{bmatrix}_0 \frac{\Delta_{2n}}{\Delta_{n+i}} \frac{\Delta_{2n}}{\Delta_{n+j}} \Delta_{i+j}$$

Proof. We use the bubble expansion formula on the top left bubble in the skein element $S_B^{(n)}(\Gamma)$ we obtain:

$$\tilde{J}_{n,\Gamma}(A) \doteq_{4(n+1)} \sum_{i=0}^n \begin{bmatrix} n & n \\ n & n \end{bmatrix}_i \begin{array}{c} \text{Diagram showing the bubble expansion of the top-left bubble. The bubble is now labeled } n-i \text{ and } i. \text{ The rest of the diagram remains the same.} \end{array}$$

Using properties of the Jones-Wenzl projector

$$\tilde{J}_{n,\Gamma}(A) \doteq_{4(n+1)} \sum_{i=0}^n \begin{bmatrix} n & n \\ n & n \end{bmatrix}_i \begin{array}{c} \text{Diagram showing the result of applying the Jones-Wenzl projector. The top-left bubble is now labeled } n-i \text{ and } i. \text{ The rest of the diagram remains the same.} \end{array}$$

Using the identity (2.4)

$$\tilde{J}_{n,\Gamma}(A) \doteq_{4(n+1)} \sum_{i=0}^n \left[\begin{array}{cc} n & n \\ n & n \end{array} \right]_i \frac{\Delta_{2n}}{\Delta_{n+i}} \cdot \text{Diagram}$$

Now apply the bubble expansion formula to the lower mostright bubble

$$\tilde{J}_{n,\Gamma}(A) \doteq_{4(n+1)} \sum_{i=0}^n \sum_{j=0}^n \left[\begin{array}{cc} n & n \\ n & n \end{array} \right]_i \left[\begin{array}{cc} n & n \\ n & n \end{array} \right]_j \frac{\Delta_{2n}}{\Delta_{n+i}} \cdot \text{Diagram 1}$$

$$= \sum_{i=0}^n \sum_{j=0}^n \left[\begin{array}{cc} n & n \\ n & n \end{array} \right]_i \left[\begin{array}{cc} n & n \\ n & n \end{array} \right]_j \frac{\Delta_{2n}}{\Delta_{n+i}} \frac{\Delta_{2n}}{\Delta_{n+j}} \cdot \text{Diagram 2}$$

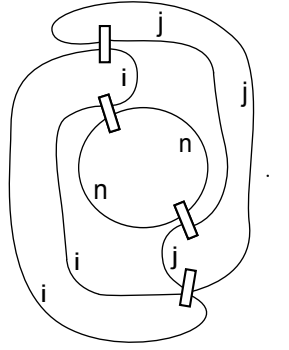
Similarly, we apply the bubble expansion formula on the top bubble that appears in the previous equation

$$\begin{aligned}
\tilde{J}_{n,\Gamma}(A) &\doteq_{4(n+1)} \sum_{i=0}^n \sum_{j=0}^n \sum_{k=0}^{\min(j,n-i)} \begin{bmatrix} n & n \\ n & n \end{bmatrix}_i \begin{bmatrix} n & n \\ n & n \end{bmatrix}_j \begin{bmatrix} j & n \\ n & n-i \end{bmatrix}_k \\
&\times \frac{\Delta_{2n}}{\Delta_{n+i}} \frac{\Delta_{2n}}{\Delta_{n+j}} \begin{array}{c} \text{Diagram 1: A vertical stack of four rectangular nodes. The top node is labeled 'j-k'. The second node is labeled 'i+k' and 'k'. The third node is labeled 'n-k' and 'n'. The bottom node is labeled 'n' and 'n-j'. Curved lines connect the nodes: a line from 'i+k' to 'j-k' labeled 'j', a line from 'n-k' to 'j-k' labeled 'j', a line from 'n-k' to 'n' labeled 'i', and a line from 'n' to 'n-j' labeled 'i'. } \end{array} \\
&= \sum_{i=0}^n \sum_{j=0}^n \sum_{k=0}^{\min(j,n-i)} \begin{bmatrix} n & n \\ n & n \end{bmatrix}_i \begin{bmatrix} n & n \\ n & n \end{bmatrix}_j \begin{bmatrix} j & n \\ n & n-i \end{bmatrix}_k \\
&\times \frac{\Delta_{2n}}{\Delta_{n+i}} \frac{\Delta_{2n}}{\Delta_{n+j}} \begin{array}{c} \text{Diagram 2: Similar to Diagram 1, but with an additional curved line from 'i+k' to 'n-k' labeled 'i'. } \end{array} .
\end{aligned}$$

Note that the previous sum is zero unless $k = 0$. Hence

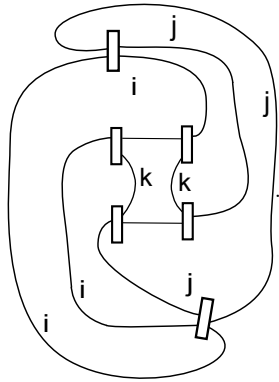
$$\tilde{J}_{n,\Gamma}(A) \doteq_{4(n+1)} \sum_{i=0}^n \sum_{j=0}^n \begin{bmatrix} n & n \\ n & n \end{bmatrix}_i \begin{bmatrix} n & n \\ n & n \end{bmatrix}_j \begin{bmatrix} j & n \\ n & n-i \end{bmatrix}_0 \frac{\Delta_{2n}}{\Delta_{n+i}} \frac{\Delta_{2n}}{\Delta_{n+j}} \begin{array}{c} \text{Diagram 3: Similar to Diagram 1, but with an additional curved line from 'i+k' to 'n-k' labeled 'i'. } \end{array} .$$

Similarly

$$\tilde{J}_{n,\Gamma}(A) \doteq_{4(n+1)} \sum_{i=0}^n \sum_{j=0}^n \begin{bmatrix} n & n \\ n & n \end{bmatrix}_i \begin{bmatrix} n & n \\ n & n \end{bmatrix}_j \begin{bmatrix} i & n \\ n & n-j \end{bmatrix}_0 \begin{bmatrix} j & n \\ n & n-i \end{bmatrix}_0 \frac{\Delta_{2n}}{\Delta_{n+i}} \frac{\Delta_{2n}}{\Delta_{n+j}}$$


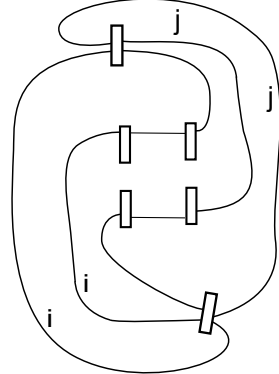
Applying the bubble expansion one last time on the middle bubble in previous summation, we obtain

$$\tilde{J}_{n,\Gamma}(A) \doteq_{4(n+1)} \sum_{i=0}^n \sum_{j=0}^n \sum_{k=0}^{\min(i,j)} \begin{bmatrix} n & n \\ n & n \end{bmatrix}_i \begin{bmatrix} n & n \\ n & n \end{bmatrix}_j \begin{bmatrix} i & n \\ n & n-j \end{bmatrix}_0 \begin{bmatrix} j & n \\ n & n-i \end{bmatrix}_0 \begin{bmatrix} j & i \\ n & n \end{bmatrix}_k$$

$$\times \frac{\Delta_{2n}}{\Delta_{n+i}} \frac{\Delta_{2n}}{\Delta_{n+j}}$$


The previous summation is zero unless $k = 0$. Hence

$$\tilde{J}_{n,\Gamma}(A) \doteq_{4(n+1)} \sum_{i=0}^n \sum_{j=0}^n \begin{bmatrix} n & n \\ n & n \end{bmatrix}_i \begin{bmatrix} n & n \\ n & n \end{bmatrix}_j \begin{bmatrix} i & n \\ n & n-j \end{bmatrix}_0 \begin{bmatrix} j & n \\ n & n-i \end{bmatrix}_0 \begin{bmatrix} j & i \\ n & n \end{bmatrix}_0$$

$$\times \frac{\Delta_{2n}}{\Delta_{n+i}} \frac{\Delta_{2n}}{\Delta_{n+j}}$$


which implies that

$$\tilde{J}_{n,\Gamma}(A) \doteq_{4(n+1)} \sum_{i=0}^n \sum_{j=0}^n \begin{bmatrix} n & n \\ n & n \end{bmatrix}_i \begin{bmatrix} n & n \\ n & n \end{bmatrix}_j \begin{bmatrix} i & n \\ n & n-j \end{bmatrix}_0 \begin{bmatrix} j & n \\ n & n-i \end{bmatrix}_0 \begin{bmatrix} j & i \\ n & n \end{bmatrix}_0 \frac{\Delta_{2n}}{\Delta_{n+i}} \frac{\Delta_{2n}}{\Delta_{n+j}} \Delta_{i+j}. \quad (4.14)$$

□

In the next proposition we work with the variable q . Recall that $A^4 = q$.

Proposition 4.23.

$$T_{\Gamma}(q) = (q; q)_{\infty}^2 \sum_{k=0}^{\infty} \frac{q^{k+k^2}}{(q; q)_k} \left(\sum_{i=0}^k q^{(-2i(k-i))} \begin{bmatrix} k \\ i \end{bmatrix}_q \right)^2.$$

Proof. Using Corollary 4.16 and the fact that

$$\prod_{i=0}^j [n-i] = q^{(2+3j+j^2-2n-2jn)/4} (1-q)^{-1-j} \frac{(q; q)_n}{(q; q)_{n-j-1}}. \quad (4.15)$$

One obtains:

$$\begin{bmatrix} n & n \\ n & n \end{bmatrix}_i = (-1)^{i+n} q^{(2i+4i^2-2n)/4} \frac{(q; q)_n^6 (q; q)_{3n-i+1}}{(q; q)_{2n}^2 (q; q)_{2n+1} (q; q)_i^2 (q; q)_{n-i}^3}, \quad (4.16)$$

and

$$\begin{bmatrix} j & n \\ n & n-i \end{bmatrix}_0 = (-1)^{n-i} q^{(i-n)/2} \frac{(q; q)_{i+j} (q; q)_n (q; q)_{n+i} (q; q)_{2n+j+1}}{(q; q)_i (q; q)_{2n} (q; q)_{j+n} (q; q)_{n+j+i+1}}. \quad (4.17)$$

Finally Lemma 4.17 implies

$$\begin{bmatrix} i & j \\ n & n \end{bmatrix}_0 \Delta_{i+j} = \Lambda(n, i, j), \quad (4.18)$$

and one could use (5.16) and the formula for the theta graph given in [19] or [25] to write

$$\begin{bmatrix} i & j \\ n & n \end{bmatrix}_0 \Delta_{i+j} = (-1)^{i+j+n} q^{-(i+j+n)/2} \frac{(q; q)_n (q; q)_j (q; q)_i (q; q)_{n+j+i+1}}{(1-q) (q; q)_{i+n} (q; q)_{j+n} (q; q)_{j+i}}. \quad (4.19)$$

Putting (4.17), (4.18), and (4.19) in (4.14) we obtain

$$\tilde{J}_{n,\Gamma}(q) \doteq_n \sum_{i=0}^n \sum_{j=0}^n P(n, i, j), \quad (4.20)$$

where

$$P(n, i, j) = \frac{(-1)^{i+j+n} q^{\frac{i}{2}+i^2+\frac{j}{2}+j^2-\frac{5n}{2}} (q; q)_{i+j} (q; q)_n^{15} (q; q)_{1+i+2n} (q; q)_{1+j+2n} (q; q)_{1-i+3n} (q; q)_{1-j+3n}}{(1-q)(q; q)_i^2 (q; q)_j^2 (q; q)_{2n}^6 (q; q)_{n-i}^3 (q; q)_{i+n} (q; q)_{n-j}^3 (q; q)_{j+n} (q; q)_{1+i+j+n} (q; q)_{1+2n}^2} \frac{\Delta_{2n}}{\Delta_{n+i}} \frac{\Delta_{2n}}{\Delta_{n+j}}.$$

Now

$$\begin{aligned} \frac{(q; q)_n}{(q; q)_{2n}} &= \frac{\prod_{i=0}^{n-1} (1 - q^{i+1})}{\prod_{i=0}^{2n-1} (1 - q^{i+1})} \\ &= \frac{1}{\prod_{i=n}^{2n-1} (1 - q^{i+1})} \\ &= \prod_{i=0}^{n-1} \frac{1}{(1 - q^{i+n+1})} \doteq_n 1. \end{aligned}$$

Similarly,

$$\frac{(q; q)_n}{(q; q)_{2n+1}} \doteq_n 1.$$

Moreover,

$$\frac{(q; q)_{3n-i+1}}{(q; q)_{2n+1}} = 1 - q^{2n+2} + O(2n+3) =_n 1.$$

and

$$\begin{aligned} \frac{(q; q)_{2n+i+1}}{(q; q)_{n+i}} &= \frac{\prod_{k=0}^{3n+i} (1 - q^{k+1})}{\prod_{i=0}^{n+i-1} (1 - q^{k+1})} \\ &= \prod_{i=n+i}^{3n+i} (1 - q^{k+1}) \doteq_n 1. \end{aligned}$$

Hence,

$$\sum_{i=0}^n \sum_{j=0}^n P(n, i, j) \doteq_n \sum_{i=0}^n \sum_{j=0}^n \frac{q^{i+i^2+j+j^2} (q; q)_{i+j} (q; q)_n^8}{(1-q)(q; q)_i^2 (q; q)_j^2 (q; q)_{n-i}^3 (q; q)_{n-j}^3}.$$

Further simplification yields:

$$\begin{aligned} \sum_{i=0}^n \sum_{j=0}^n \frac{q^{i+i^2+j+j^2}(q; q)_{i+j}(q; q)_n^8}{(1-q)(q; q)_i^2(q; q)_j^2(q; q)_{n-i}^3(q; q)_{n-j}^3} &\stackrel{=}{=} (q; q)_n^2 \sum_{i=0}^n \sum_{j=0}^n \frac{q^{i+i^2+j+j^2}(q; q)_{i+j}}{(1-q)(q; q)_i^2(q; q)_j^2} \\ &= \frac{(q; q)_n^2}{(1-q)} \sum_{i=0}^n \sum_{k=i}^n \frac{q^{k+k^2-2i(k-i)}}{(q; q)_k} \left[\begin{matrix} k \\ i \end{matrix} \right]_q^2. \end{aligned}$$

The definition of the quantum binomial coefficients allows us to write

$$\frac{(q; q)_n^2}{(1-q)} \sum_{i=0}^n \sum_{k=i}^n \frac{q^{k+k^2-2i(k-i)}}{(q; q)_k} \left[\begin{matrix} k \\ i \end{matrix} \right]_q^2 = \frac{(q; q)_n^2}{1-q} \sum_{k=0}^n \frac{q^{k+k^2}}{(q; q)_k} \left(\sum_{i=0}^k q^{(-2i(k-i))} \left[\begin{matrix} k \\ i \end{matrix} \right]_q^2 \right).$$

Hence

$$T_\Gamma(q) \stackrel{=}{=} \frac{\tilde{J}_{n,\Gamma}(q)}{\Delta_n(q)} \stackrel{=}{=} (q; q)_\infty^2 \sum_{k=0}^\infty \frac{q^{k+k^2}}{(q; q)_k} \left(\sum_{i=0}^k q^{(-2i(k-i))} \left[\begin{matrix} k \\ i \end{matrix} \right]_q^2 \right).$$

□

Using Mathematica we computed the first 120 terms of $T_\Gamma(q)$:

$$\begin{aligned} T_{85} \stackrel{=}{=} & 1 - 2q + q^2 - 2q^4 + 3q^5 - 3q^8 + q^9 + 4q^{10} - q^{11} - 2q^{12} - 2q^{13} - 3q^{14} + 3q^{15} + \\ & 7q^{16} + 2q^{17} - 4q^{18} - 4q^{19} - 4q^{20} - 5q^{21} + 3q^{22} + 9q^{23} + 9q^{24} - 4q^{26} - 9q^{27} - 8q^{28} - \\ & 5q^{29} - q^{30} + 9q^{31} + 13q^{32} + 16q^{33} + 5q^{34} - 10q^{35} - 13q^{36} - 15q^{37} - 12q^{38} - 7q^{39} + \\ & 15q^{41} + 25q^{42} + 23q^{43} + 15q^{44} - 3q^{45} - 16q^{46} - 28q^{47} - 31q^{48} - 21q^{49} - 12q^{50} + 4q^{51} + \\ & 16q^{52} + 37q^{53} + 41q^{54} + 39q^{55} + 26q^{56} - 6q^{57} - 34q^{58} - 48q^{59} - 51q^{60} - 49q^{61} - 32q^{62} - \\ & 8q^{63} + 20q^{64} + 39q^{65} + 67q^{66} + 76q^{67} + 67q^{68} + 43q^{69} + 9q^{70} - 36q^{71} - 74q^{72} - 99q^{73} - \\ & 101q^{74} - 79q^{75} - 52q^{76} - 7q^{77} + 33q^{78} + 77q^{79} + 108q^{80} + 135q^{81} + 127q^{82} + 104q^{83} + \\ & 51q^{84} - 10q^{85} - 82q^{86} - 145q^{87} - 174q^{88} - 182q^{89} - 160q^{90} - 115q^{91} - 37q^{92} + 37q^{93} + \end{aligned}$$

$$\begin{aligned}
& 119q^{94} + 177q^{95} + 218q^{96} + 238q^{97} + 229q^{98} + 171q^{99} + 88q^{100} - 17q^{101} - 126q^{102} - \\
& 236q^{103} - 313q^{104} - 344q^{105} - 325q^{106} - 256q^{107} - 157q^{108} - 28q^{109} + 98q^{110} + 241q^{111} + \\
& 343q^{112} + 420q^{113} + 440q^{114} + 424q^{115} + 336q^{116} + 212q^{117} + 41q^{118} - 150q^{119} - 324q^{120}.
\end{aligned}$$

Chapter 5

The Tail of a Quantum Spin Network and Roger-Ramanujan Type Identities

5.1 Introduction

In this chapter we generalize the study of the tail of the colored Jones polynomial to study the tail of certain trivalent graphs in S^2 . In particular, we study the tail of a sequence of admissible trivalent graphs with edges colored n or $2n$. We use local skein relations to understand and compute the tail of these graphs. We also give product formulas for the tail of such trivalent graphs. Finally, we show that our skein theoretic techniques naturally lead to a proof for the Andrews-Gordon identities for the two variable Ramanujan theta function as well to corresponding new identities for the false theta function. This chapter is based on our work in [10].

Skein theoretic techniques have been used in [3] and [4] to understand the head and tail of an adequate link. It was proven in [3] that for an adequate link L the first $(n+1)$ coefficients of n^{th} unreduced colored Jones polynomial, considering the q variable, coincide with the first $(n+1)$ coefficients of the evaluation in $\mathcal{S}(S^2)$ of a certain skein element in S^2 . We demonstrate here that this skein element can be realized as quantum spin network obtained from the link diagram D . Hence, studying the tail of the colored Jones polynomial can be reduced to studying the tail of these quantum spin networks.

A quantum spin network is a banded trivalent graph with edges labeled by non-negative integers, also called the colors of the edges, and the three edges meeting at a vertex satisfy some admissibility conditions. The main purpose of this chapter

is to understand the tail of a sequence of planer quantum spin network with edges colored n or $2n$. Our method to study the tail of such graphs relies mainly on adapting various skein theoretic identities to new ones that can in turn be used to compute and understand the tail of such graphs. Studying the tail of these graphs via local skein relations does not only give an intuitive method to compute the tails but also demonstrates certain equivalence between the tails of different quantum spin networks as well as the existence of the tail of graphs that are not necessarily derived from alternating links.

The q -series obtained from knots in this way appear to be connected to classical number theoretic identities. Hikami [14] realized that that Rogers-Ramanujan identities appear in the study of the colored Jones polynomial of torus knots. In [4] Armond and Dasbach calculate the head and the tail of the colored Jones polynomial via multiple methods and use these computations to prove number theoretic identities. In this chapter we show that the skein theoretic techniques we developed herein can be also used to prove classical identities in number theory. In particular we use skein theory to prove the Andrews-Gordon identities for the two variable Ramanujan theta function, as well as corresponding identities for the false theta function.

5.2 Background

In this section we give the definitions of the general Ramanujan theta function and false theta functions and we list some of their properties.

5.2.1 Roger Ramanujan type identities

1. The general two variable Ramanujan theta function, see [2], is defined by :

$$f(a, b) = \sum_{i=0}^{\infty} a^{i(i+1)/2} b^{i(i-1)/2} + \sum_{i=1}^{\infty} a^{i(i-1)/2} b^{i(i+1)/2} \quad (5.1)$$

The definition of $f(a, b)$ implies

$$f(a, b) = f(b, a).$$

The Jacobi triple product identity of $f(a, b)$ is given by

$$f(a, b) = (-a; ab)_\infty (-b, ab)_\infty (ab, ab)_\infty,$$

It follows immediately from the Jacobi triple product identity that

$$f(-q^2, -q) = (q; q)_\infty.$$

The function $f(a, b)$ specializes to (5.1)

$$f(-q^{2k}, -q) = \sum_{i=0}^{\infty} (-1)^i q^{k(i^2+i)} q^{i(i-1)/2} + \sum_{i=1}^{\infty} (-1)^i q^{k(i^2-i)} q^{i(i+1)/2}. \quad (5.2)$$

The Andrews-Gordon identity for the Ramanujan theta function is given by

$$f(-q^{2k}, -q) = (q, q)_\infty \sum_{l_1=0}^{\infty} \sum_{l_2=0}^{\infty} \cdots \sum_{l_{k-1}=0}^{\infty} \frac{q^{\sum_{j=1}^{k-1} (i_j(i_j+1))}}{\prod_{j=1}^{k-1} (q, q)_{l_j}} \quad (5.3)$$

where $i_j = \sum_{s=j}^{k-1} l_s$. This identity is a generalization of the second Rogers-Ramanujan identity

$$f(-q^4, -q) = (q, q)_\infty \sum_{i=0}^{\infty} \frac{q^{i^2+i}}{(q, q)_i} \quad (5.4)$$

2. The general two variable Ramanujan false theta function is given by (e.g. [23]):

$$\Psi(a, b) = \sum_{i=0}^{\infty} a^{i(i+1)/2} b^{i(i-1)/2} - \sum_{i=1}^{\infty} a^{i(i-1)/2} b^{i(i+1)/2} \quad (5.5)$$

In particular

$$\Psi(q^{2k-1}, q) = \sum_{i=0}^{\infty} q^{ki^2+(k-1)i} - \sum_{i=1}^{\infty} q^{k(i^2-i)+i} \quad (5.6)$$

We will show that the Andrews-Gordon identities (5.3) have corresponding identities for the false Ramanujan theta function:

$$\Psi(q^{2k-1}, q) = (q, q)_\infty \sum_{l_1=0}^{\infty} \sum_{l_2=0}^{\infty} \cdots \sum_{l_{k-1}=0}^{\infty} \frac{q^{\sum_{j=1}^{k-1} (i_j(i_j+1))}}{(q, q)_{l_{k-1}}^2 \prod_{j=1}^{k-2} (q, q)_{l_j}} \quad (5.7)$$

where $i_j = \sum_{s=j}^{k-1} l_s$. The latter identity is a generalization of the following identity (Ramanujan's notebook, Part III, Entry 9 [6])

$$\Psi(q^3, q) = (q, q)_\infty \sum_{i=0}^{\infty} \frac{q^{i^2+i}}{(q; q)_i^2} \quad (5.8)$$

Using skein theory, we recover and prove the identities (5.3) and (5.7) in Theorem 5.27.

5.3 Existence of the Tail of an Adequate Skein Element

In [3] C. Armond proves that the tail of the colored Jones polynomial of alternating links exist. This was done by proving that the tail of the colored Jones polynomial of an alternating link L is equal to the tail a sequence of certain skein elements in $\mathcal{S}(S^2)$ obtained from an alternating link diagram of L . In fact, Armond proved this for a larger class of links, called Adequate links. Following [3], we briefly recall the proof of existence of the tail the colored Jones polynomial and we illustrate how this can be applied to our study.

Every alternating link L induces a family of adequate skein elements in S^2 . Let D be an alternating diagram of L . These adequate skein elements are the skein elements $S_B^{(n)}(D)$ that we introduced in the previous chapter. Armond proved that the tail of family $\{S_B^{(n)}(D)\}_{n \in \mathbb{N}}$ exists by showing that $S_B^{(n+1)}(D)(q) \doteq_{n+1} S_B^{(n)}(D)(q)$ using three basic steps:

1. Since the link diagram D is alternating one can observe that $S_B^{(n+1)}(D)$ is an adequate skein element and it actually looks locally like Figure 5.1.

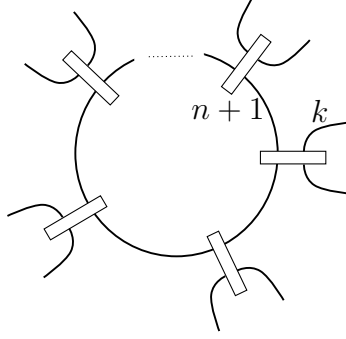
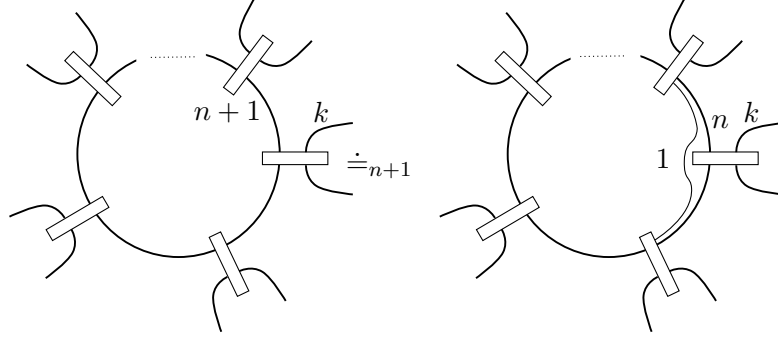


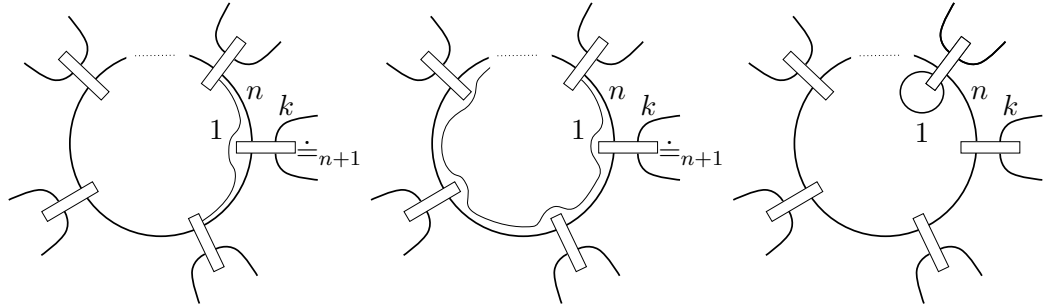
FIGURE 5.1. A local picture for $S_B^{(n+1)}(D)$

Furthermore, we have the following equality



This is done by using the recursive definition of the Jones-Wenzl idempotent and showing that all of the other terms resulting from applying the recursive definition of the idempotent do not contribute to the first $n + 1$ coefficients of $S_B^{(n+1)}(D)$.

2. Step one can be applied around the circle until we reach the final idempotent:



and finally one can show that removing the circle colored 1 do not affect the first $n + 1$ coefficients of $S_B^{(n+1)}(D)$.

3. Step one and two can be applied on every circle in $S_B^{(n+1)}(D)$ and eventually we reduce $S_B^{(n+1)}(D)$ to $S_B^{(n)}(D)$.

Now let $\mathcal{D} = \{D_n(q)\}_{n \in \mathbb{N}}$ be a sequence of skein elements in $\mathcal{S}(S^2)$. The previous discussion implies that the tail of the sequence \mathcal{D} exists whenever the skein elements $D_n(q)$ are adequate. On the other hand, we know that the tail of the sequence \mathcal{D} exists if and only if $D_{n+1}(q) \doteq_n D_n(q)$. This condition and the previous proof suggest that adequateness of every diagram in the family \mathcal{D} may be a necessary condition for the tail of \mathcal{D} to exist. This is not true however, and in the next section we give infinite family of sequences of inadequate skein elements whose tail exist. See Example 5.17.

5.4 Computing the Tail of a Quantum Spin Network Via Local Skein Relations

Let D be a planer trivalent graph. Recall that an admissible coloring of D is an assignment of colors to the edges of D so that at each vertex, the three colors meeting there form an admissible triple. Consider a sequence of admissible quantum spin networks $\{D_n\}_{n \in \mathbb{N}}$ obtained from D by labeling each edge by n or $2n$. Recall that the evaluation of the quantum spin network D_n in the skein module $\mathcal{S}(S^2)$ gives in general a rational function. Using definition 3.1 and remark 3.2 one could study the tail of the sequence $\{D_n\}_{n \in \mathbb{N}}$. In this section we will study the tail of such skein elements. We start this section with a simple calculation for a certain coefficient of a crossingless matching diagram in the expansion of the Jones-Wenzl projector and we use this coefficient to derive our first local skein relation. We then use the bubble skein relation to compute more complicated local skein relations.

Remark 5.1. *Since we will be working closely with identities such as the bubble expansion equation it will be easier to work with Jones-Wenzl projectors than to work with trivalent graphs. For this reason we will not state our results in terms of trivalent graphs notation.*

One can regard any skein element Γ in the linear skein space T_{a_1, a_2, \dots, a_m} as an element of the dual space $T_{a_1, a_2, \dots, a_m}^*$. This is done by embedding the space T_{a_1, a_2, \dots, a_m} in S^2 and wiring the outside in some way to obtain a skein element in $\mathcal{S}(S^2)$. Let Γ be an element of the skein space T_{a_1, a_2, \dots, a_m} and let x be a wiring in the disk in S^2 that is complementary to T_{a_1, a_2, \dots, a_m} with the same specified boundary points. Denote by Γ^* to the element in $T_{a_1, a_2, \dots, a_m}^*$ induced by the skein element Γ . We call the skein element $\Gamma^*(x) \in \mathcal{S}(S^2)$ a *closure* of Γ . In the following definition we assume that α_n and β_n are admissible trivalent graphs with edges labeled n or $2n$ in the skein space T_{a_1, a_2, \dots, a_m} , where $a_i \in \{n, 2n\}$, with α_n^* and β_n^* are the corresponding dual elements.

Definition 5.2. *Let $\alpha_n, \beta_n, \alpha_n^*$ and β_n^* be as above. Let S be a subset of T_{a_1, a_2, \dots, a_m} . We say that*

$$\alpha_n \doteq_n \beta_n$$

on S if

$$\alpha_n^*(x) \doteq_n \beta_n^*(x)$$

for all x in S .

Remark 5.3. *The set S mentioned in the definition can be chosen to be the set of all wiring x such that the skein elements $\alpha_n^*(x)$ and $\beta_n^*(x)$ are adequate. However, adequateness seems to be unnecessary in some cases and one could loosen this condition on the set S further. We will give examples of such cases in this chapter. Ideally, the set S is supposed to be the set of all wiring x such that the tail of the skein elements $\alpha_n^*(x)$ and $\beta_n^*(x)$ exist. It is not known to the author what is the largest set for which this condition holds.*

Remark 5.4. *If we are working with $T_{a,b,c}$, where $(a, b, c) \in \{(2n, 2n, 2n), (n, n, 2n)\}$, then for any skein element α_n in $T_{a,b,c}$ we can write*

$$\alpha_n = P_n(q)\tau_{a,b,c} \quad (5.9)$$

for some rational function $P_n(q)$. Hence if x is an element in $T_{a,b,c}$ then the tail of the sequence $\{\alpha_n^(x)\}_{n \in \mathbb{N}}$ exists if and only if the tails of the sequences $\{\tau_{a,b,c}^*(x)\}_{n \in \mathbb{N}}$ and $\{P_n(q)\}_{n \in \mathbb{N}}$ exist. In particular, 5.9 also implies that if the tail of $\{P_n(q)\}_{n \in \mathbb{N}}$ exists and x is a wiring in $T_{a,b,c}$ such that $\tau_{a,b,c}^*(x)$ is an adequate skein element, then the tail of the sequence $\{\alpha_n^*(x)\}_{n \in \mathbb{N}}$ exists. Note that for every such x one has $P_n(q) \doteq_n \alpha_n^*(x)/\tau_{a,b,c}^*(x)$.*

Following Morrison [27], write $\text{coeff}_{\in f^{(n)}}(D)$ to denote the coefficient of the crossing-less matching diagram D appearing in the n^{th} Jones-Wenzl projector. We will use Morrison's recursive formula to calculate certain coefficients of the Jones-Wenzl idempotent. The recursive formula is explained very well in [27], see Proposition 4.1 and the examples within, and we shall not repeat it here.

Lemma 5.5.

$$\text{coeff}_{\in f^{(2n)}} \left(\begin{array}{c} \text{Diagram with two crossings and } n \text{ strands} \end{array} \right) = \frac{([n]!)^2}{[2n]!} \quad (5.10)$$

Proof. Applying Morrison's induction formula, Proposition 4.1 in [27], on the left hand side of (5.10), we obtain

$$\begin{aligned}
\text{coeff}_{\in f^{(2n)}} \left(\text{diagram} \right) &= \frac{[n]}{[2n]} \text{coeff}_{\in f^{(2n-1)}} \left(\text{diagram} \right) \\
&= \frac{[n][n-1]}{[2n][2n-1]} \text{coeff}_{\in f^{(2n-2)}} \left(\text{diagram} \right) \\
&= \frac{[n]!}{\prod_{i=n+1}^{2n} [i]} = \frac{([n]!)^2}{[2n]!}
\end{aligned}$$

□

Proposition 5.6. *For all adequate closures of the element $\tau_{n,n,2n}$ and for all $n \geq 0$:*

$$\begin{array}{c} \text{diagram} \end{array} \stackrel{\cdot}{=} (q; q)_n \begin{array}{c} \text{diagram} \end{array} \quad (5.11)$$

Proof. Write Γ_n to denote the skein element that appears on the left hand side of 5.11.

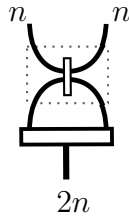


FIGURE 5.2. Expanding $f^{(2n)}$

Consider the idempotent $f^{(2n)}$ that appears in Γ_n inside the square in Figure 5.2 and expand this element as a $\mathbb{Q}(A)$ -linear summation of crossingless matching diagrams. Every crossingless matching diagram in this expansion, except for the diagram that appears in Figure 5.3, is going to produce a hook to the bottom

idempotent $f^{(2n)}$ in Γ_n and hence the term with such crossingless matching diagram evaluates to zero.

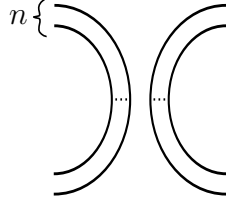


FIGURE 5.3. A crossingless matching that appears in the expansion of $f^{(2n)}$

This allows us to write

$$\begin{aligned}
 \begin{array}{c} n \quad n \\ \text{Diagram: a cup shape with a vertical line through its center} \\ 2n \end{array} &= \text{coeff}_{\in f^{(2n)}} \left(\begin{array}{c} \text{Diagram: two sets of } n \text{ parallel arcs} \\ n \end{array} \right) \begin{array}{c} n \quad n \\ \text{Diagram: a cup shape with a vertical line through its center} \\ 2n \end{array} \\
 &= \frac{([n]!)^2}{[2n]!} \begin{array}{c} n \quad n \\ \text{Diagram: two cups side-by-side} \\ 2n \end{array}
 \end{aligned}$$

Using the fact $[n]! = q^{(n-n^2)/4}(1-q)^{-n}(q, q)_n$ we can write

$$\begin{aligned}
 \frac{([n]!)^2}{[2n]!} &= q^{n^2/2} \frac{(q; q)_n^2}{(q; q)_{2n}} \\
 &= q^{n^2/2} \frac{\left(\prod_{i=0}^{n-1} (1 - q^{i+1}) \right)^2}{\prod_{i=0}^{2n-1} (1 - q^{i+1})} \\
 &= q^{n^2/2} \frac{\prod_{i=0}^{n-1} (1 - q^{i+1})}{\prod_{i=n}^{2n-1} (1 - q^{i+1})}.
 \end{aligned}$$

However,

$$q^{n^2/2} \prod_{i=0}^{n-1} \frac{(1 - q^{i+1})}{(1 - q^{i+n+1})} \doteq_n \prod_{i=0}^{n-1} (1 - q^{i+1}) = (q; q)_n$$

□

Proposition 5.7. *For all adequate closures of the element $\tau_{n,n,2n}$ and for all $n \geq 0$:*

$$\begin{array}{c} \text{Diagram 1: A cup with two strands labeled } n \text{ entering from the sides, a horizontal bar at the bottom labeled } 2n, \text{ and a small circle at the top labeled } n. \\ \hline \text{Diagram 2: A cup with two strands labeled } n \text{ entering from the sides, a horizontal bar at the bottom labeled } 2n, \text{ and no top circle.} \end{array} \doteq_n (q; q)_n \quad (5.12)$$

Proof.

$$\begin{array}{c} \text{Diagram 1: Same as Diagram 1 in (5.12).} \\ \hline \text{Diagram 2: A cup with two strands labeled } n \text{ entering from the sides, a horizontal bar at the bottom labeled } 2n, \text{ and a small circle at the top labeled } n. \end{array} = \sum_{i=0}^n \begin{bmatrix} n & n \\ n & n \end{bmatrix}_i \begin{array}{c} \text{Diagram 3: A cup with two strands labeled } n \text{ entering from the sides, a horizontal bar at the bottom labeled } 2n, \text{ and a small circle at the top labeled } i. \\ \hline \text{Diagram 4: A cup with two strands labeled } n \text{ entering from the sides, a horizontal bar at the bottom labeled } 2n, \text{ and no top circle.} \end{array} = \begin{bmatrix} n & n \\ n & n \end{bmatrix}_0 \begin{array}{c} \text{Diagram 4: Same as Diagram 4 in the previous equation.} \end{array}$$

The first equation follows by applying the bubble expansion formula, Theorem 4.11, and the second equation follows from the annihilation axiom of the Jones-Wenzl idempotent.

Using (??) and the fact that

$$\prod_{i=0}^j [n - i] = q^{(2+3j+j^2-2n-2jn)/4} (1 - q)^{-1-j} \frac{(q; q)_n}{(q; q)_{n-j-1}} \quad (5.13)$$

we can write

$$\begin{bmatrix} n & n \\ n & n \end{bmatrix}_0 = (-1)^n q^{-n/2} \frac{(q; q)_n^3 (q; q)_{3n+1}}{(q; q)_{2n}^2 (q; q)_{2n+1}}. \quad (5.14)$$

However,

$$\frac{(q; q)_{3n+1}}{(q; q)_{2n+1}} = 1 - q^{2n+2} + O(2n+3) =_n 1,$$

and

$$\frac{(q; q)_n}{(q; q)_{2n}} =_n 1,$$

hence (5.14) yields:

$$\left[\begin{array}{cc} n & n \\ n & n \end{array} \right]_0 \doteq_n (q; q)_n,$$

and the result follows. \square

Remark 5.8. In [10] we showed that

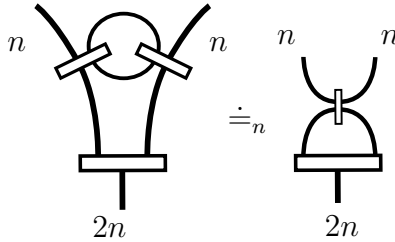
$$\left[\begin{array}{cc} n & n \\ n & n \end{array} \right]_0 \Delta_{2n} = \Theta(2n, 2n, 2n).$$

Hence the previous theorem implies

$$\Theta(2n, 2n, 2n) \doteq_n \frac{(q, q)_n}{1 - q} = (q^2, q)_n.$$

Propositions 5.6 and 5.7 imply immediately the following result.

Proposition 5.9. For all adequate closures of the left hand side skein element of the following equation and for all $n \geq 0$ the following holds:



Lemma 5.10. For $n \geq 1$:

$$1. \sum_{i=0}^n \left[\begin{array}{cc} n & n \\ n & n \end{array} \right]_i \frac{\Delta_{2n}}{\Delta_{n+i}} \doteq_n \Psi(q^3, q).$$

$$2. \sum_{i=0}^n \begin{bmatrix} n & n \\ n & n \end{bmatrix}_i \begin{bmatrix} n & i \\ n & n \end{bmatrix}_0 \frac{\Delta_{2n}}{\Delta_{n+i}} \doteq_n f(-q^4, -q).$$

Proof. 1. Set $P(n, i) := \begin{bmatrix} n & n \\ n & n \end{bmatrix}_i \frac{\Delta_{2n}}{\Delta_{n+i}}$. From the bubble expansion formula, Theorem 4.11, we obtain,

$$P(n, i) = q^{i(i-n)/2} \frac{[2n+1]}{[n+i+1]} \frac{\prod_{j=0}^{n-i-1} [n-j] \prod_{s=0}^{i-1} [n-s]^2}{\prod_{h=0}^{n-1} [2n-h]^2} \binom{n}{i}_q \prod_{k=0}^{n-i-1} [3n-i-k+1] \quad (5.15)$$

Using (??) and the fact that

$$\prod_{i=0}^j [n-i] = q^{(2+3j+j^2-2n-2jn)/4} (1-q)^{-1-j} \frac{(q; q)_n}{(q; q)_{n-j-1}}, \quad (5.16)$$

we can rewrite (5.15) to obtain the following:

$$P(n, i) = q^{(2i+4i^2-2n)/4} \frac{[2n+1]}{[n+i+1]} \frac{(q; q)_n^6 (q; q)_{3n-i+1}}{(q; q)_{2n}^2 (q; q)_{2n+1} (q; q)_i^2 (q; q)_{n-i}^3}. \quad (5.17)$$

Now we shall study the first n terms of $P(n, i+1) + P(n, i)$. We claim that

$$P(n, i) + P(n, i+1) \doteq_n P(n, i) + Q(n, i+1),$$

where $\frac{(q; q)_n}{(q; q)_{n-i}} Q(n, i) = P(n, i)$. To prove this claim observe first that $m(P(n, i)) = (i + i^2 - n)$. Note also that for all $1 \leq i \leq n$:

$$\frac{(q; q)_n}{(q; q)_{n-i}} = 1 + O(n - i + 1).$$

This implies that the minimal degree of $Q(n, i)$ is equal to the minimal degree of $P(n, i)$. Thus

$$\begin{aligned}
P(n, i) + P(n, i + 1) &= P(n, i) + \frac{(q, q)_n}{(q, q)_{n-i-1}} Q(n, i + 1) \\
&= P(n, i) + (1 + O(n - i)) Q(n, i + 1) \\
&= P(n, i) + Q(n, i + 1) + O(2 + 2i + i^2) \\
&\doteq_n P(n, i) + Q(n, i + 1).
\end{aligned}$$

The last equation is true since $m(P(n, i) + P(n, i + 1)) = i + i^2 - n$ and hence the terms $O(3 + 2i + i^2)$ do not contribute the first n terms of $P(n, i) + P(n, i + 1)$ for every $i \geq 0$. This proves our claim and hence we can write:

$$\begin{aligned}
P(n, 0) + P(n, 2) + \dots + P(n, n) &\doteq_n P(n, 0) + \dots + P(n, n - 1) + Q(n, n) \\
&\doteq_n P(n, 0) + Q(n, 2) \dots + Q(n, n - 1) + Q(n, n) \\
&= Q(n, 0) + Q(n, 2) \dots + Q(n, n - 1) + Q(n, n).
\end{aligned}$$

The last equality follows from the fact that $P(n, 0) = Q(n, 0)$. We can prove similarly that

$$\sum_{i=0}^n P(n, i) \doteq_n \sum_{i=0}^n Q'(n, i),$$

where $\frac{(q; q)_n^3}{(q; q)_{n-i}^3} Q'(n, i) = P(n, i)$. Using this result and (5.17) we obtain

$$\sum_{i=0}^n P(n, i) \doteq_n \sum_{i=0}^n q^{(i/2+i^2)} \frac{[2n+1]}{[n+i+1]} \frac{(q; q)_n^3 (q; q)_{3n-i+1}}{(q; q)_{2n}^2 (q; q)_{2n+1} (q; q)_i^2}. \quad (5.18)$$

Now

$$\frac{(q; q)_{3n-i+1}}{(q; q)_{2n+1}} = 1 - q^{2n+2} + O(2n+3) =_n 1, \quad (5.19)$$

and similarly we can show that

$$\frac{(q, q)_n}{(q, q)_{2n}} =_n 1. \quad (5.20)$$

Putting (5.19) and (5.20) all in (5.18) we obtain:

$$\begin{aligned}
\sum_{i=0}^n P(n, i) &\doteq_n (q; q)_n \sum_{i=0}^n \frac{q^{i/2+i^2}}{(q; q)_i^2} \frac{[2n+1]}{[n+i+1]} \\
&\doteq_n (q; q)_n \sum_{i=0}^n \frac{q^{i+i^2}}{(q; q)_i^2} \\
&\doteq_n \Psi(q^3, q).
\end{aligned}$$

2. Using 5.16 one can write

$$\left[\begin{array}{cc} n & i \\ n & n \end{array} \right]_0 = (-1)^n q^{-n/2} \frac{(q; q)_i (q; q)_n^2 (q; q)_{2n+i+1}}{(q; q)_{n+i+1} (q; q)_{n+i} (q; q)_{2n}}. \quad (5.21)$$

Equations 5.15 and 5.21 imply:

$$\left[\begin{array}{cc} n & n \\ n & n \end{array} \right]_i \left[\begin{array}{cc} n & i \\ n & n \end{array} \right]_0 \frac{\Delta_{2n}}{\Delta_{n+i}} = (-1)^n q^{i/2+i^2-n} \frac{[2n+1]}{[n+i+1]} \times \frac{(q; q)_n^8 (q; q)_{2n+i+1} (q; q)_{3n-i+1}}{(q; q)_{n+i+1} (q; q)_{n+i} (q; q)_{n-i}^3 (q; q)_i (q; q)_{2n}^3 (q; q)_{2n+1}}.$$

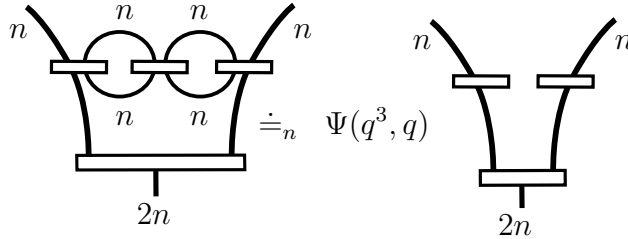
Using similar calculations to the ones we did in (1), one can write

$$\sum_{i=0}^n \left[\begin{array}{cc} n & n \\ n & n \end{array} \right]_i \left[\begin{array}{cc} n & i \\ n & n \end{array} \right]_0 \frac{\Delta_{2n}}{\Delta_{n+i}} \doteq_n (q; q)_n \sum_{i=0}^n \frac{q^{i^2+i}}{(q; q)_i} \doteq_n f(-q^4, -q).$$

□

Proposition 5.11. *For adequate closures of the element $\tau_{n,n,2n}$ and for all $n \geq 0$:*

1.



2.

The diagram shows an equality between two expressions. On the left, a diagram with a base labeled $2n$ and four external lines labeled n . It contains two bubbles, each with two internal lines labeled n . On the right, the same base and external lines are shown, but the bubbles are replaced by two separate components, each consisting of a horizontal bar and a vertical line. The expression $f(-q^4, -q)$ is placed between the two diagrams.

Proof. 1. Applying the bubble expansion formula on the left bubble, we obtain,

The diagram shows an equality between two expressions. On the left, a diagram with a base labeled $2n$ and four external lines labeled n . It contains two bubbles, each with two internal lines labeled n . On the right, the same base and external lines are shown, but the left bubble is expanded into a sum over i from 0 to n . Each term in the sum is a diagram with a base labeled $2n$ and four external lines labeled n . The left bubble is replaced by a diagram with two internal lines labeled i and $n-i$. The expression $f(-q^4, -q)$ is placed between the two diagrams.

Using the property (2.4) of the idempotent, we obtain

The diagram shows an equality between two expressions. On the left, a diagram with a base labeled $2n$ and four external lines labeled n . It contains two bubbles, each with two internal lines labeled n . On the right, the same base and external lines are shown, but the left bubble is expanded into a sum over i from 0 to n . Each term in the sum is a diagram with a base labeled $2n$ and four external lines labeled n . The left bubble is replaced by a diagram with two internal lines labeled i and $n-i$. The expression $f(-q^4, -q)$ is placed between the two diagrams.

Using Lemma 5.10 (1) we obtain

The diagram shows an equality between two expressions. On the left, a diagram with a base labeled $2n$ and four external lines labeled n . It contains two bubbles, each with two internal lines labeled n . On the right, the same base and external lines are shown, but the left bubble is replaced by a diagram with two internal lines labeled n and n . The expression $\Psi(q^3, q)$ is placed between the two diagrams.

2. Using the bubble expansion formula on the left most bubble we obtain:

$$\begin{aligned}
 \text{Diagram 1} &= \sum_{i=0}^n \begin{bmatrix} n & n \\ n & n \end{bmatrix}_i \text{Diagram 2} \\
 &= \sum_{i=0}^n \begin{bmatrix} n & n \\ n & n \end{bmatrix}_i \text{Diagram 3}
 \end{aligned}$$

Diagram 1: A cup-like structure with a base labeled $2n$. It has four external strands labeled n . Inside, there are three bubbles. The top bubble is connected to the two middle bubbles by two strands labeled n . Each of the two middle bubbles is connected to the base by a strand labeled n .

Diagram 2: Similar to Diagram 1, but the top bubble is expanded. It has two external strands labeled i and $n-i$ entering from the left and right respectively. The two middle bubbles remain connected to the base by strands labeled n .

Diagram 3: Similar to Diagram 2, but the top bubble is further expanded. It has two external strands labeled i and j entering from the left and right respectively. The two middle bubbles remain connected to the base by strands labeled n .

Using (2.4) we can write the previous equation as:

$$\begin{aligned}
 \text{Diagram 1} &= \sum_{i=0}^n \begin{bmatrix} n & n \\ n & n \end{bmatrix}_i \frac{\Delta_{2n}}{\Delta_{n+i}} \text{Diagram 2} \\
 &= \sum_{i=0}^n \sum_{j=0}^i \begin{bmatrix} n & n \\ n & n \end{bmatrix}_i \begin{bmatrix} n & i \\ n & n \end{bmatrix}_j \frac{\Delta_{2n}}{\Delta_{n+i}} \text{Diagram 3}
 \end{aligned}$$

Diagram 2: Similar to Diagram 1, but the top bubble is expanded. It has two external strands labeled i and $n-i$ entering from the left and right respectively. The two middle bubbles remain connected to the base by strands labeled n .

Diagram 3: Similar to Diagram 2, but the top bubble is further expanded. It has two external strands labeled i and j entering from the left and right respectively. The two middle bubbles remain connected to the base by strands labeled n .

Hence,

$$\text{Diagram 1} = \sum_{i=0}^n \sum_{j=0}^i \begin{bmatrix} n & n \\ n & n \end{bmatrix}_i \begin{bmatrix} n & i \\ n & n \end{bmatrix}_j \frac{\Delta_{2n}}{\Delta_{n+i}} \text{Diagram 2}$$

Diagram 1: Same as in the previous equation.

Diagram 2: Similar to Diagram 1, but the top bubble is expanded. It has two external strands labeled i and j entering from the left and right respectively. The two middle bubbles remain connected to the base by strands labeled n .

The skein element in the on the right of the previous equation is zero unless $j = 0$. Hence, Lemma 5.10 (2) yields the result.

□

More generally we have the following theorem.

Theorem 5.12. *For all adequate closures of the element $\tau_{n,n,2n}$ and for all $n, k \geq 1$:*

1.

$$\begin{array}{c}
 \text{Diagram with } 2k \text{ bubbles} \\
 \text{Diagram with } 2n \text{ strands} \\
 \text{Diagram with } 2n \text{ strands}
 \end{array}
 \stackrel{\cdot}{=}
 (q, q)_n \sum_{l_1=0}^n \sum_{l_2=0}^n \dots \sum_{l_k=0}^n \frac{q^{\sum_{j=1}^k (i_j(i_j+1))}}{(q, q)_{l_k}^2 \prod_{j=1}^{k-1} (q, q)_{l_j}}
 \begin{array}{c}
 \text{Diagram with } 2n \text{ strands} \\
 \text{Diagram with } 2n \text{ strands}
 \end{array}$$

where $i_j = \sum_{s=j}^k l_s$.

2.

$$\begin{array}{c}
 \text{Diagram with } 2k+1 \text{ bubbles} \\
 \text{Diagram with } 2n \text{ strands} \\
 \text{Diagram with } 2n \text{ strands}
 \end{array}
 \stackrel{\cdot}{=}
 (q, q)_n \sum_{l_1=0}^n \sum_{l_2=0}^n \dots \sum_{l_k=0}^n \frac{q^{\sum_{j=1}^k (i_j(i_j+1))}}{\prod_{j=1}^k (q, q)_{l_j}}
 \begin{array}{c}
 \text{Diagram with } 2n \text{ strands} \\
 \text{Diagram with } 2n \text{ strands}
 \end{array}$$

where $i_j = \sum_{s=j}^k l_s$.

Proof. 1. We proceed as in the previous theorem and we apply the bubble expansion formula on the left most bubble we obtain:

$$\begin{array}{c}
 \text{Diagram with } 2k \text{ bubbles} \\
 \text{Diagram with } 2n \text{ strands}
 \end{array}
 = \sum_{i_1=0}^n \begin{bmatrix} n & n \\ n & n \end{bmatrix}_{i_1}
 \begin{array}{c}
 \text{Diagram with } 2n \text{ strands} \\
 \text{Diagram with } 2n \text{ strands}
 \end{array}$$

$$= \sum_{i_1=0}^n \begin{bmatrix} n & n \\ n & n \end{bmatrix}_{i_1} \frac{\Delta_{2n}}{\Delta_{n+i_1}}
 \begin{array}{c}
 \text{Diagram with } 2k-2 \text{ bubbles} \\
 \text{Diagram with } 2n \text{ strands}
 \end{array}$$

Each time we apply the bubble expansion formula we eliminate two bubbles. Hence, after k applications of the bubble expansion formula we obtain:

The diagram shows a chain of $2k$ bubbles, each with two external legs labeled n . The chain is connected by horizontal lines. Below the chain is a thick horizontal bar labeled $2n$. This is equated to a sum over indices i_1, i_2, \dots, i_{k-1} of a product of k terms, each being a 2×2 matrix $\begin{bmatrix} n & n \\ n & n \end{bmatrix}_{i_j}$ multiplied by a fraction $\frac{\Delta_{2n}}{\Delta_{n+i_1}}$. This is then multiplied by a single 2×2 matrix $\begin{bmatrix} n & i_{j-1} \\ n & n \end{bmatrix}_{i_j}$. The result is a diagram of a V-shaped structure with two external legs labeled n at the top and a thick horizontal bar labeled $2n$ at the bottom. A fraction $\frac{\Delta_{2n}}{\Delta_{n+i_j}}$ is placed to the left of the V-shape.

Using 5.16 we can compute

$$\begin{bmatrix} n & i \\ n & n \end{bmatrix}_j = (-1)^{j+n} q^{j^2+j/2-n/2} \frac{(q, q)_i^2 (q, q)_n^4 (q, q)_{2n+i-j+1}}{(q, q)_{i-j} (q, q)_j^2 (q, q)_{2n} (q, q)_{n+i} (q, q)_{n+i+1} (q, q)_{n-j}^2}$$

Similar calculations to the ones we did in Lemma 5.10 implies:

$$\begin{aligned} & \sum_{i_1=0}^n \sum_{i_2=0}^{i_1} \dots \sum_{i_k=0}^{i_{k-1}} \begin{bmatrix} n & n \\ n & n \end{bmatrix}_{i_1} \frac{\Delta_{2n}}{\Delta_{n+i_1}} \prod_{j=2}^k \begin{bmatrix} n & i_{j-1} \\ n & n \end{bmatrix}_{i_j} \frac{\Delta_{2n}}{\Delta_{n+i_j}} \doteq_n \\ & (q, q)_n \sum_{i_1=0}^n \sum_{i_2=0}^{i_1} \dots \sum_{i_k=0}^{i_{k-1}} \frac{q^{\sum_{j=1}^k (i_j(i_j+1))}}{(q, q)_{i_k}^2 \prod_{j=2}^k (q, q)_{i_{j-1}-i_j}} \end{aligned}$$

The previous summation can be written as

$$\begin{aligned} & (q, q)_n \sum_{i_1=0}^n \sum_{i_2=0}^{i_1} \dots \sum_{i_k=0}^{i_{k-1}} \frac{q^{\sum_{j=1}^k (i_j(i_j+1))}}{(q, q)_{i_k}^2 \prod_{j=2}^k (q, q)_{i_{j-1}-i_j}} = \\ & (q, q)_n \sum_{i_k=0}^n \sum_{i_{k-1}=i_k}^n \dots \sum_{i_1=i_2}^n \frac{q^{\sum_{j=1}^k (i_j(i_j+1))}}{(q, q)_{i_k}^2 \prod_{j=2}^k (q, q)_{i_{j-1}-i_j}} \end{aligned}$$

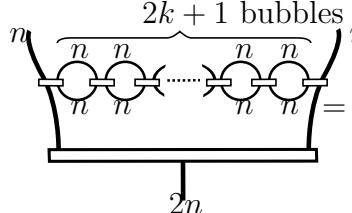
Now if we set $l_j = i_j - i_{j+1}$ for $j = 1, \dots, k-1$ and $l_k = i_k$, we obtain $i_j = \sum_{s=j}^k l_s$ and hence we can rewrite the right side of the previous equation as

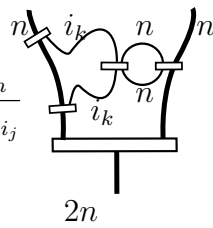
$$(q, q)_n \sum_{i_k=0}^n \sum_{i_{k-1}=i_k}^n \cdots \sum_{i_1=i_2}^n \frac{q^{\sum_{j=1}^k (i_j(i_j+1))}}{(q, q)_{i_k}^2 \prod_{j=2}^k (q, q)_{i_{j-1}-i_j}} =$$

$$(q, q)_n \sum_{l_1=0}^n \sum_{l_2=0}^n \cdots \sum_{l_k=0}^n \frac{q^{\sum_{j=1}^k (i_j(i_j+1))}}{(q, q)_{l_k}^2 \prod_{j=1}^{k-1} (q, q)_{l_j}}$$

where $i_j = \sum_{s=j}^k l_s$. Hence the result follows.

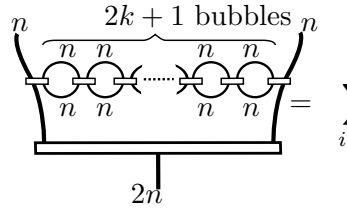
2. We apply the bubble expansion formula k times we obtain: small

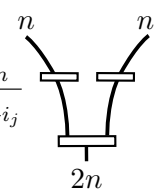


$$= \sum_{i_1=0}^n \sum_{i_2=0}^{i_1} \cdots \sum_{i_k=0}^{i_{k-1}} \begin{bmatrix} n & n \\ n & n \end{bmatrix}_{i_1} \frac{\Delta_{2n}}{\Delta_{n+i_1}} \prod_{j=2}^k \begin{bmatrix} n & i_{j-1} \\ n & n \end{bmatrix}_{i_j}$$


$$\times \frac{\Delta_{2n}}{\Delta_{n+i_j}}$$

Hence,



$$= \sum_{i_1=0}^n \sum_{i_2=0}^{i_1} \cdots \sum_{i_k=0}^{i_{k-1}} \begin{bmatrix} n & n \\ n & n \end{bmatrix}_{i_1} \begin{bmatrix} n & i_k \\ n & n \end{bmatrix}_0 \frac{\Delta_{2n}}{\Delta_{n+i_1}} \prod_{j=2}^k \begin{bmatrix} n & i_{j-1} \\ n & n \end{bmatrix}_{i_j}$$


$$\times \frac{\Delta_{2n}}{\Delta_{n+i_j}}$$

and one can do computations to the coefficient in the last equation similar to the ones we did in Lemma 5.10 and obtain:

$$\sum_{i_1=0}^n \sum_{i_2=0}^{i_1} \dots \sum_{i_k=0}^{i_{k-1}} \begin{bmatrix} n & n \\ n & n \end{bmatrix}_{i_1} \begin{bmatrix} n & i_k \\ n & n \end{bmatrix}_0 \frac{\Delta_{2n}}{\Delta_{n+i_1}} \prod_{j=2}^k \begin{bmatrix} n & i_{j-1} \\ n & n \end{bmatrix}_{i_j} \frac{\Delta_{2n}}{\Delta_{n+i_j}} \doteq_n$$

$$(q, q)_n \sum_{i_1=0}^n \sum_{i_2=0}^{i_1} \dots \sum_{i_k=0}^{i_{k-1}} \frac{q^{\sum_{j=1}^k (i_j(i_j+1))}}{(q, q)_{i_k} \prod_{j=2}^k (q, q)_{i_{j-1}-i_j}}$$

The previous summation can be rewritten as follows:

$$(q, q)_n \sum_{i_1=0}^n \sum_{i_2=0}^{i_1} \dots \sum_{i_k=0}^{i_{k-1}} \frac{q^{\sum_{j=1}^k (i_j(i_j+1))}}{(q, q)_{i_k} \prod_{j=2}^k (q, q)_{i_{j-1}-i_j}} =$$

$$(q, q)_n \sum_{i_k=0}^n \sum_{i_{k-1}=i_k}^n \dots \sum_{i_1=i_2}^n \frac{q^{\sum_{j=1}^k (i_j(i_j+1))}}{(q, q)_{i_k} \prod_{j=2}^k (q, q)_{i_{j-1}-i_j}}$$

Set $l_j = i_j - i_{j+1}$ for $j = 1, \dots, k-1$ and $l_k = i_k$, we obtain $i_j = \sum_{s=j}^k l_s$ and hence we can rewrite the previous equation:

$$(q, q)_n \sum_{i_k=0}^n \sum_{i_{k-1}=i_k}^n \dots \sum_{i_1=i_2}^n \frac{q^{\sum_{j=1}^k (i_j(i_j+1))}}{(q, q)_{i_k} \prod_{j=2}^k (q, q)_{i_{j-1}-i_j}} = (q, q)_n \sum_{l_1=0}^n \sum_{l_2=0}^n \dots \sum_{l_k=0}^n \frac{q^{\sum_{j=1}^k (i_j(i_j+1))}}{\prod_{j=1}^k (q, q)_{l_j}}$$

where $i_j = \sum_{s=j}^k l_s$.

□

Corollary 5.13. *For all adequate closures of the element $f^{(n)}$ and for all $n, k \geq 1$:*

1.

$$\left. \begin{array}{c} n \\ \vdots \\ n \end{array} \right\} 2k+1 \text{ bubbles} \doteq_n (q, q)_n \sum_{l_1=0}^n \sum_{l_2=0}^n \dots \sum_{l_k=0}^n \frac{q^{\sum_{j=1}^k (i_j(i_j+1))}}{(q, q)_{l_k}^2 \prod_{j=1}^{k-1} (q, q)_{l_j}} \quad \begin{array}{c} n \\ \text{---} \square \text{---} \\ n \end{array}$$

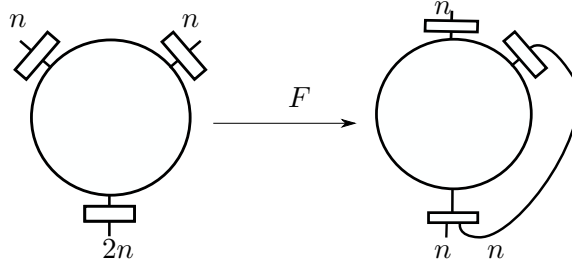
$$\text{where } i_j = \sum_{s=j}^k l_s.$$

2.

$$\left\{ \begin{array}{c} n \\ \text{2k bubbles} \\ n \\ \vdots \\ n \\ n \end{array} \right\} \doteq_n (q, q)_n \sum_{l_1=0}^n \sum_{l_2=0}^n \cdots \sum_{l_{k-1}=0}^n \frac{q^{\sum_{j=1}^{k-1} (i_j(i_j+1))}}{\prod_{j=1}^{k-1} (q, q)_{l_j}} \quad \begin{array}{c} n \\ \boxed{} \\ n \end{array}$$

$$\text{where } i_j = \sum_{s=j}^{k-1} l_s.$$

Proof. (1) Let $F : T_{n,n,2n} \longrightarrow T_{n,n}$ be the wiring linear map defined by



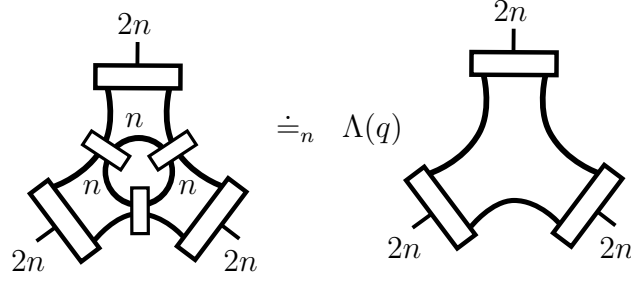
This map is clearly an isomorphism. The result follows by noticing that

$$F \left(\begin{array}{c} n \\ \text{2k bubbles} \\ n \\ \vdots \\ n \\ n \end{array} \right) = \begin{array}{c} n \\ \text{2k+1 bubbles} \\ n \\ \vdots \\ n \\ n \end{array}$$

(2) The proof is similar to (1). □

The previous theorem and its corollary give an interesting proof of the Andrews-Gordon identities for the theta function and corresponding identities for the false theta function. We give this proof in section 5.6.

Theorem 5.14. *For all adequate closures of the element $\tau_{2n,2n,2n}$ and for all $n \geq 0$:*

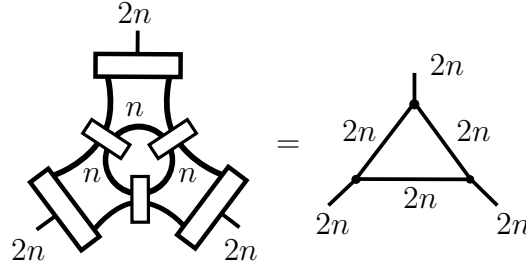


$$\stackrel{\cdot}{=}_n \Lambda(q)$$

where

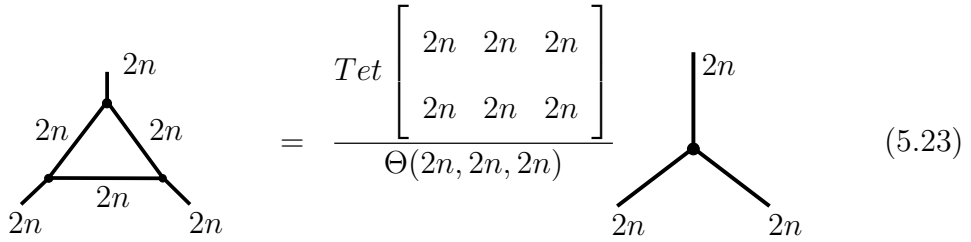
$$\Lambda(q) = (q; q)_\infty^2 \sum_{i=0}^{\infty} \frac{(-1)^i q^{(i+3i^2)/2}}{(q; q)_i^3} \quad (5.22)$$

Proof. First note that



$$=$$

and hence



$$= \frac{Tet \begin{bmatrix} 2n & 2n & 2n \\ 2n & 2n & 2n \end{bmatrix}}{\Theta(2n, 2n, 2n)} \quad (5.23)$$

As before we only have to show:

$$\frac{Tet \begin{bmatrix} 2n & 2n & 2n \\ 2n & 2n & 2n \end{bmatrix}}{\Theta(2n, 2n, 2n)} \stackrel{\cdot}{=} \Lambda(q)$$

To this end, note first that the bubble expansion formula implies

$$\Theta(2n, 2n, 2n) = \begin{bmatrix} n & n \\ n & n \end{bmatrix}_0 \Delta_{2n} = q^{-n/2} \frac{(q; q)_n^3 (q; q)_{3n+1}}{(q; q)_{2n}^2 (q; q)_{2n+1}} [2n + 1].$$

and hence Theorem 5.7 implies

$$\Theta(2n, 2n, 2n) \doteq_n \frac{(q; q)_n}{(1 - q)} \quad (5.24)$$

On the other hand one could use the Tetrahedron coefficient formula in [25] to obtain

$$Tet \begin{bmatrix} 2n & 2n & 2n \\ 2n & 2n & 2n \end{bmatrix} = \frac{([n]!)^{12}}{([2n]!)^6} \sum_{i=3n}^{4n} \frac{(-1)^i [i+1]!}{([4n-i]!)^3 ([i-3n]!)^4}. \quad (5.25)$$

Using the identity

$$\prod_{i=0}^j [n-i] = q^{(2+3j+j^2-2n-2jn)/4} (1-q)^{-1-j} \frac{(q; q)_n}{(q; q)_{n-j-1}}$$

the equation (5.25) can be written as

$$Tet \begin{bmatrix} 2n & 2n & 2n \\ 2n & 2n & 2n \end{bmatrix} = \frac{q^{3n^2} (q; q)_n^{12}}{(q; q)_{2n}^6} \sum_{i=3n}^{4n} \frac{(-1)^{1+3n+i} q^{-i/2+3i^2/2-12in+21n^2} (q, q)_{i+1}}{(1-q)(q, q)_{i-3n}^4 (q, q)_{4n-i}^3}$$

One can simplify the previous equation to obtain

$$Tet \begin{bmatrix} 2n & 2n & 2n \\ 2n & 2n & 2n \end{bmatrix} = \frac{q^{-2n} (q; q)_n^{12}}{(q; q)_{2n}^6} \sum_{i=0}^n \frac{(-1)^i q^{(i+3i^2)/2} (q, q)_{4n-i}}{(1-q)(q, q)_{n-i}^4 (q, q)_i^3}$$

Using the same techniques we used in Lemma 5.10 we can write

$$Tet \begin{bmatrix} 2n & 2n & 2n \\ 2n & 2n & 2n \end{bmatrix} \doteq_n (q; q)_n^3 \sum_{i=0}^{\infty} \frac{(-1)^i q^{(i+3i^2)/2}}{(1-q)(q; q)_i^3} \quad (5.26)$$

Putting (5.24) and (5.26) in (5.23) yield the result. \square

Remark 5.15. *The tail of the tetrahedron whose edges all colored $2n$ is computed in the previous theorem, see equation (5.26). The tail of this element can be seen to be $\Lambda(q)(q^2; q)_n$. This tail was also computed by Garoufalidis and Le in [8].*

Example 5.16. All edges in the following graphs are colored $2n$.

$$\begin{array}{c}
 \text{Diagram 1} \stackrel{\cdot}{\equiv}_n \Lambda(q) \\
 \stackrel{\cdot}{\equiv}_n \Lambda^2(q)(q^2; q)_\infty
 \end{array}
 \text{Diagram 2}$$

The first equation follows from the previous theorem and the second one follows from the same theorem and remark 5.8.

Example 5.17. All arcs in the following skein elements are colored n .

$$\begin{array}{c}
 \text{Diagram 1} \stackrel{\cdot}{\equiv}_n (q, q)_\infty \\
 \stackrel{\cdot}{\equiv}_n (q, q)_\infty^2
 \end{array}
 \text{Diagram 2}$$

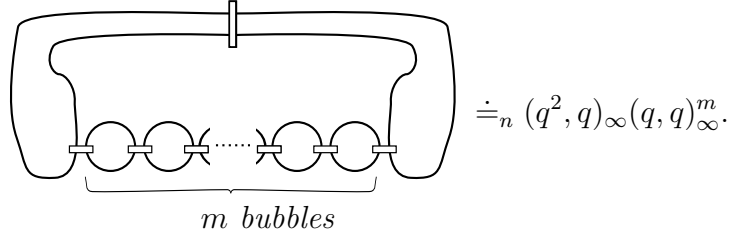
The first and the second equations follow from Proposition 5.6. Observe that Proposition 5.6 also implies

$$\text{Det} \begin{bmatrix} 2n & n & n \\ 2n & n & n \end{bmatrix} = \text{Diagram 1} \stackrel{\cdot}{\equiv}_n (q, q)_n \text{Diagram 2} \stackrel{\cdot}{\equiv}_n \frac{(q, q)_n}{1-q} \stackrel{\cdot}{\equiv}_n (q^2; q)_n.$$

Hence,

$$\text{Diagram 1} \stackrel{\cdot}{\equiv}_n (q^2, q)_\infty (q, q)_\infty^2.$$

Similarly, one can compute



Note that the skein elements in this example are all inadequate. In particular the skein elements $Tet \begin{bmatrix} 2n & n & n \\ 2n & n & n \end{bmatrix}$ is inadequate.

5.5 Tail Multiplication Structures on Quantum Spin Networks

In [4] C. Armond and O. Dasbach defined a product structure on the tail of the color Jones polynomial. In this section we will define a few product structures on the tail of trivalent graphs in $\mathcal{S}(S^2)$ using similar techniques to the ones in [4]. Let Γ_1 and Γ_2 be trivalent graphs in $\mathcal{S}(S^2)$. Suppose that each of Γ_1 and Γ_2 contains the trivalent graph $\tau_{2n,2n,2n}$ as in Figure 5.4.

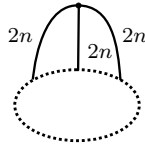


FIGURE 5.4. The graph Γ with a trivalent graph $\tau_{2n,2n,2n}$

Define the map

$$[,]_1 : \mathcal{S}(S^2) \times \mathcal{S}(S^2) \longrightarrow \mathcal{S}(S^2)$$

via the wiring map shown below.

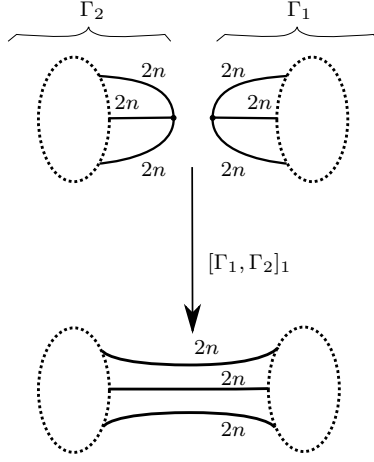


FIGURE 5.5. The product $[\Gamma_1, \Gamma_2]_1$

The proof of the following theorem is analogous to the proof of Theorem 5.1 in [4].

Theorem 5.18. *Let Γ_1 and Γ_2 as defined above. Suppose further that T_{Γ_1} and T_{Γ_2} exist. Then*

$$[\Gamma_1, \Gamma_2]_1 \doteq_n \frac{1}{(q^2, q)_n} T_{\Gamma_1} T_{\Gamma_2}$$

Proof. If you regard the element $\tau_{2n, 2n, 2n}$ as a map of the outside, then the fact that the space $T_{2n, 2n, 2n}$ is one dimensional generated by the the graph $\tau_{2n, 2n, 2n}$ allows us to write

$$\Gamma_i = f_i(q) \Theta(2n, 2n, 2n),$$

where $f_i(q) \in \mathbb{Q}(q)$ for $i = 1, 2$. On the other hand one can also use the same fact to write

$$[\hat{\Gamma}_1, \hat{\Gamma}_2]_1 = f_1(q) f_2(q) \Theta(2n, 2n, 2n).$$

By assumption we have

$$T_{\hat{\Gamma}_i} \doteq_n f_i(q) \Theta(2n, 2n, 2n)$$

for $i = 1, 2$. Hence

$$\begin{aligned}
[\hat{\Gamma}_1, \hat{\Gamma}_2]_1 &\doteq_n T_{\hat{\Gamma}_1} \frac{T_{\hat{\Gamma}_2}}{\Theta(2n, 2n, 2n)} \\
&\doteq_n \frac{1}{(q^2, q)_n} T_{\hat{\Gamma}_1} T_{\hat{\Gamma}_2}
\end{aligned}$$

□

Similarly, suppose that Υ_1 and Υ_2 are trivalent graphs in $\mathcal{S}(S^2)$ and each of them contains the idempotent $f^{(2n)}$ as in Figure 5.6. Suppose further that Ξ_1 and Ξ_2 are trivalent graphs in $\mathcal{S}(S^2)$ and each of them contains the idempotent $f^{(n)}$ as shown in Figure 5.6 below.



FIGURE 5.6. The graph Υ (left) and the graph Ξ (right)

Define the maps

$$[\cdot, \cdot]_i : \mathcal{S}(S^2) \times \mathcal{S}(S^2) \longrightarrow \mathcal{S}(S^2)$$

for $i = 2, 3$ as shown below.

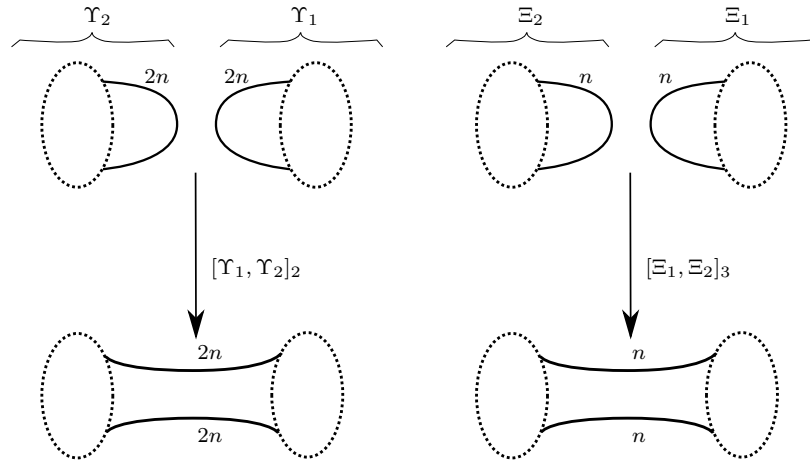


FIGURE 5.7. The product $[\Upsilon_1, \Upsilon_2]_2$ (left) and the product $[\Xi_1, \Xi_2]_3$ (right)

As before these maps induce multiplication structures on skein elements in $\mathcal{S}(S^2)$ in the following sense.

Theorem 5.19. *Suppose that Υ_1 and Υ_2 are trivalent graphs in $\mathcal{S}(S^2)$ and suppose that each of them contains the projector $f^{(n)}$ or $f^{(2n)}$ as in Figure 5.6. Suppose further that T_{Υ_1} and T_{Υ_2} exist. Then*

$$[\Upsilon_1, \Upsilon_2]_i \doteq_n (1 - q)T_{\Upsilon_1}T_{\Upsilon_2}$$

for $i = 2, 3$.

Proof. The proof follows from the fact that space $T_{a,a}$ is one dimensional generated by $f^{(a)}$ and

$$\frac{1}{\Delta_n} \doteq_n \frac{1}{\Delta_{2n}} \doteq_n 1 - q.$$

The rest of the proof is identical to the proof of 5.18. □

5.6 Applications

In this section we give two applications of the the tail of quantum spin networks. The first application we show that the tail of the colored Jones polynomial satisfies certain product structure. In our second application, we show that the skein theoretic techniques we developed in this chapter naturally lead to a proof for the Andrews-Gordon identities for the two variable Ramanujan theta function as well to corresponding new identities for the false theta function.

5.6.1 The Tail of the Colored Jones Polynomial

In [3] C. Armond and O. Dasbach introduced the tail of the colored Jones polynomial. The existence of the tail of the colored Jones polynomial of an alternating links was conjectured by Dasbach and Lin [7] and in [4] C. Armond proved that the tail of colored Jones polynomial of adequate links exists. Higher order stability of the coefficients of the colored Jones polynomial of alternating links is studied

by Garoufalidis and Le in [8]. Explicit calculations were done on the knot table to determine the tail of colored Jones polynomial of alternating links in [3]. The knot 8_5 is the first knot on the knot table whose tail could not be determined by a direct application of techniques in [3]. In the previous chapter we use theorem 4.19 and the bubble expansion formula to compute the tail of the 8_5 and we gave an explicit formula for it. In this section we apply the results we obtain in section 5.4 to study the tail of the color Jones polynomial.

Remark 5.20. *When dealing with the tail of colored Jones polynomial of a link L we usually compute the tail of normalized polynomial $\tilde{J}_{n,L}(q)/\Delta_n(q)$. We will adapt this convention in this section.*

Let L be an alternating link in S^3 and let D be a reduced alternating diagram of L . Recall from section 5.3 that the skein elements $\{S_B^{(n)}(D)\}_{n \in \mathbb{N}}$ are obtained from all- B smoothing Kauffman state of D . See Figure 4.5. Recall from the previous chapter that the tail of the unreduced colored Jones polynomial of an alternating link only depends on the reduced B -graph. See also 4.19.

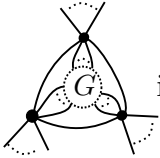
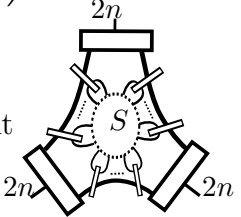
Remark 5.4 implies the following important result.

Theorem 5.21. (1) *Let G be the graph shown on the right hand side of the following identity, then there exists a q -power series $A(q)$ series such that*

$$T \left(\text{Diagram 1} \right) \doteq_n A(q) T \left(\text{Diagram 2} \right) \quad (5.27)$$

(2) (Armond and Dasbach [3]) Let G' be the graph shown on the right hand side of the following identity, then there exists a q -power series $A'(q)$ series such that

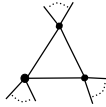
$$T \left(\text{graph } G' \right) \stackrel{=}{=} A'(q) T \left(\text{graph } \begin{array}{c} \bullet \text{---} \bullet \\ \diagup \quad \diagdown \end{array} \right) \quad (5.28)$$

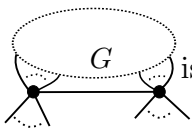
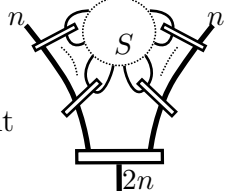
Proof. (1) The graph  is equivalent to the skein element  in the skein module $T_{2n,2n,2n}$. Here S is the skein element obtained from G by replacing every vertex by a circle colored n and every edge by an idempotent that connects two circles. However,

$$\text{graph } S \stackrel{=}{=} f_n(q) \text{graph } \begin{array}{c} \text{top box} \\ \diagup \quad \diagdown \\ \text{bottom box} \end{array} \quad (5.29)$$

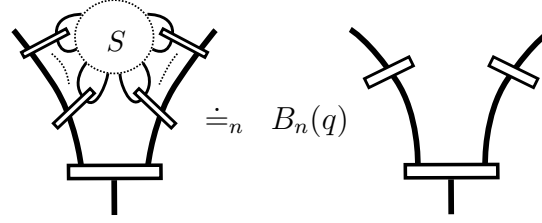
for some rational function $f_n(q)$. This holds because the skein module $T_{2n,2n,2n}$ is free on the generator $\tau_{2n,2n,2n}$. Write α_n^* to denote the skein element on the left hand side of (5.29) then the result follows by noticing

$$\begin{aligned} f_n(q) &\stackrel{=}{=} \alpha_n^*(\tau_{2n,2n,2n}) / \tau_{2n,2n,2n}^*(\tau_{2n,2n,2n}) \\ &= \alpha_n^*(\tau_{2n,2n,2n}) / \theta(2n, 2n, 2n) \\ &\stackrel{=}{=} \alpha_n^*(\tau_{2n,2n,2n}) / (q^2; q)_\infty. \end{aligned}$$

Now the result follows by noticing that the graph  is equivalent to the skein element of the right hand side of (5.29).

(2) The graph  is equivalent to the skein element  in the skein module $T_{2n,n,n}$. where S is the skein element obtained from G as explained

in (1). Since the skein module $T_{2n,n,n}$ is freely generated by $\tau_{2n,n,n}$, we have



$$\text{Diagram} \doteq_n B_n(q) \text{Diagram} \quad (5.30)$$

for some rational function $B_n(q)$. However,

$$\begin{aligned} B_n(q) &\doteq_n \beta_n^*(\tau_{n,n,2n}) / \tau_{2n,n,n}^*(\tau_{2n,n,n}) \\ &= \beta_n^*(\tau_{2n,n,n}) / \theta(2n, n, n) \\ &\doteq_n \beta_n^*(\tau_{2n,n,n}). \end{aligned}$$

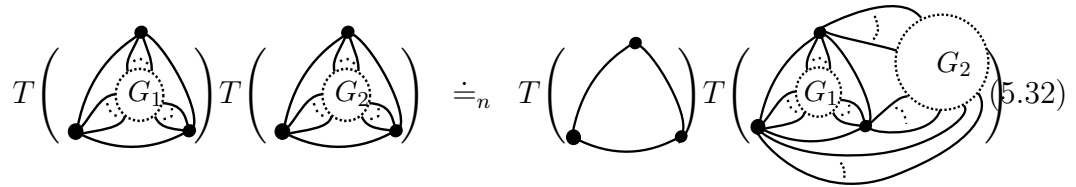
The result follows by noticing that the graph on the right hand side of (5.28) is equivalent to the skein element on the right hand side of 5.30. \square

As mentioned in the previous section, Armond and Dasbach [3] showed that if G_1 and G_2 are reduced graphs then the product of the tails T_{G_1} and T_{G_2} is equal to the tail of the graph $G_1 * G_2$ obtained from G_1 and G_2 by gluing one edge from G_1 and another edge from G_2 . In other words the following identity holds

$$T_{G_1} T_{G_2} = T_{G_1 * G_2}. \quad (5.31)$$

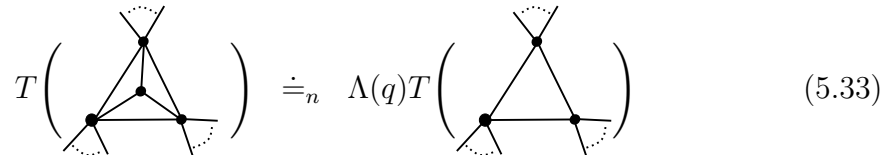
Theorem 5.21 (2) merely a restatement of this result. On the other hand, Theorem 5.21 (1) implies immediately the following result.

Corollary 5.22. *The tail of reduced graphs satisfies the following product:*



$$T(G_1) T(G_2) \doteq_n T(G_1 * G_2) \quad (5.32)$$

Note that Theorem 5.14 is a special case of 5.21 (1) and it can be stated as:



$$T(\text{Graph}) \doteq_n \Lambda(q) T(\text{Graph}) \quad (5.33)$$

The following examples illustrate how one could apply the results obtained in section 5.4 to compute the tail of a reduced graph.

Example 5.23.

$$T\left(\begin{array}{c} \bullet \\ \diagup \quad \diagdown \\ \bullet \quad \bullet \\ \diagup \quad \diagdown \quad \diagup \quad \diagdown \\ \bullet \quad \bullet \quad \bullet \\ \diagup \quad \diagdown \quad \diagup \quad \diagdown \quad \diagup \quad \diagdown \\ \bullet \quad \bullet \quad \bullet \quad \bullet \end{array}\right) \doteq_n (\Lambda(q))^4 T\left(\begin{array}{c} \bullet \\ \diagup \quad \diagdown \\ \bullet \quad \bullet \end{array}\right) \doteq_n (\Lambda(q))^4 (q; q)_\infty.$$

Where in the first equality we used equation (5.33) and in the second equality we used the fact that the tail of a triangle is the same as the tail of $\Theta(2n, 2n, 2n)$ which is just $(q^2; q)_\infty$. Recall here that we normalize tail by dividing by Δ_n . See remark 5.20.

Example 5.24. Let G_m be the reduced graph in the Figure 5.8.

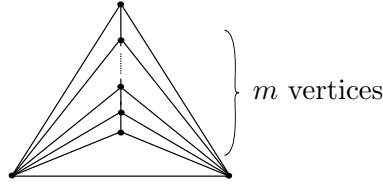


FIGURE 5.8. The graph G_m

Then the tail of this graph can be computed as follows:

$$T(G_m) \doteq_n (\Lambda(q))^m T\left(\begin{array}{c} \bullet \\ \diagup \quad \diagdown \\ \bullet \quad \bullet \end{array}\right) \doteq_n (\Lambda(q))^m (q; q)_\infty.$$

Here used again equation (5.33) in the first equality.

Example 5.25. Let $k \geq 1$ and $l \geq 0$. Let $G_{k,l}$ be the reduced graph in the Figure 5.9.

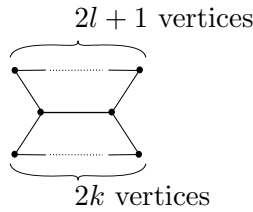


FIGURE 5.9. The graph $G_{k,l}$

Then using Theorem 5.22 one could see that

$$T(G_{k,l}) \doteq_n \Psi(q^{2k+1}, q) T \left(\overbrace{\text{Diagram}}^{2l+1 \text{ vertices}} \right) \doteq_n \Psi(q^{2k+1}, q) f(-q^{2l+2}, q).$$

Remark 5.26. Example 5.25 can be computed also using the techniques of Armond and Dasbach in [3].

5.6.2 The Tail of the Colored Jones Polynomial and Andrews-Gordon Identities

The fact that the tail of an alternating link L is a well-defined q -power series invariant implies that any two expressions of the tail of L are equal. This can be used to prove various q -identities and it was first utilized by Armond and Dasbach in [3] where they showed that the Andrews-Gordon identity for the theta function can be proven using two methods to compute the tail of the $(2, 2k+1)$ torus knots. In particular Armond and Dasbach use R -matrices and a combinatorial version of the quantum determinant formulation of Huynh and Le [13] developed by Armond [5] to compute the colored Jones polynomial of the $(2, 2k+1)$ torus knot. These computations are then used to obtain two expressions of the tail associated with the $(2, 2k+1)$ torus knot. The q -series they obtained are precisely the two sides of the Andrews-Gordon identity for the theta function. In this section we show that the skein theoretic techniques developed in this chapter can be used to prove the following false theta function identity:

$$\sum_{i=0}^{\infty} q^{ki^2+(k-1)i} - \sum_{i=1}^{\infty} q^{k(i^2-i)+i} = (q, q)_{\infty} \sum_{l_1=0}^{\infty} \sum_{l_2=0}^{\infty} \cdots \sum_{l_{k-1}=0}^{\infty} \frac{q^{\sum_{j=1}^{k-1} (i_j(i_j+1))}}{(q, q)_{l_{k-1}}^2 \prod_{j=1}^{k-2} (q, q)_{l_j}}$$

with $k \geq 2$ and $i_j = \sum_{s=j}^{k-1} l_s$.

We also show that the same skein theoretic techniques can be applied to prove the Andrews-Gordon identity for the theta function 5.3. Our techniques to prove the identity (5.3) has the advantage over the ones in [3] in that our method restricts the tools used to prove this identity to skein theory.

Denote the torus knot $(2, f)$ in Figure 5.10 by K_f .

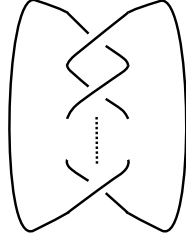


FIGURE 5.10. The $(2, f)$ torus knot

Theorem 5.27. 1. For all $k \geq 2$:

$$\sum_{i=0}^{\infty} q^{ki^2 + (k-1)i} - \sum_{i=1}^{\infty} q^{k(i^2 - i) + i} = (q, q)_{\infty} \sum_{l_1=0}^{\infty} \sum_{l_2=0}^{\infty} \cdots \sum_{l_{k-1}=0}^{\infty} \frac{q^{\sum_{j=1}^{k-1} (i_j(i_j+1))}}{(q, q)_{l_{k-1}}^2 \prod_{j=1}^{k-2} (q, q)_{l_j}}$$

$$\text{with } i_j = \sum_{s=j}^{k-1} l_s.$$

2. (The Andrews-Gordon identity for the theta function) For all $k \geq 1$

$$\begin{aligned} \sum_{i=0}^{\infty} (-1)^i q^{k(i^2+i)} q^{i(i-1)/2} + \sum_{i=1}^{\infty} (-1)^i q^{k(i^2-i)} q^{i(i+1)/2} \\ = (q, q)_{\infty} \sum_{l_1=0}^{\infty} \sum_{l_2=0}^{\infty} \cdots \sum_{l_{k-1}=0}^{\infty} \frac{q^{\sum_{j=1}^{k-1} (i_j(i_j+1))}}{\prod_{j=1}^{k-1} (q, q)_{l_j}} \end{aligned}$$

$$\text{with } i_j = \sum_{s=j}^{k-1} l_s.$$

Proof. 1. Using linear skein theory Kauffman bracket one can easily compute the colored Jones polynomial of K_f . See [18] or [22] for more details about

skein theory.

$$\tilde{J}_{n,K_f}(q)/\Delta_n(q) = \frac{1}{\Delta_n(q)} \sum_{i=0}^n (-1)^{f(n-i)} q^{f(2i+2i^2-2n-n^2)/4} \Delta_{2i}(q).$$

Hence,

$$\tilde{J}_{n,K_f}(q)/\Delta_n(q) \doteq_n \sum_{i=0}^n (-1)^{fi} q^{f(i+i^2)/2} (q^{-i} - q^{1+i}). \quad (5.34)$$

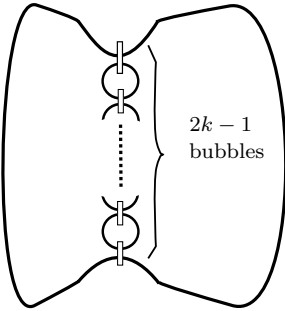
If $f = 2k$, then we can rewrite the previous equation:

$$\begin{aligned} \sum_{i=0}^n q^{2k(i+i^2)/2} (q^{-i} - q^{1+i}) &= \sum_{i=0}^n q^{-i+ik+i^2k} - \sum_{i=0}^n q^{1+i+ik+i^2k} \\ &= \sum_{i=0}^{\infty} q^{ki^2+(k-1)i} - \sum_{i=1}^{\infty} q^{k(i^2-i)+i} \end{aligned}$$

Hence

$$\tilde{J}_{n,K_{2k}}(q)/\Delta_n(q) \doteq_n \Psi(q^{2k-1}, q) \quad (5.35)$$

On the other hand theorem 4.19 implies

$$\tilde{J}_{n,K_{2k}}(q)/\Delta_n(q) \doteq_n \frac{1}{\Delta_n(q)} \left(\text{Diagram of a surface with } 2k-1 \text{ bubbles} \right)$$


and the tail of the skein element in the previous equation can be computed from corollary 5.13 and we can obtain

$$\tilde{J}_{n,K_{2k}}(q)/\Delta_n(q) \doteq_n (q, q)_n \sum_{l_1=0}^n \sum_{l_2=0}^n \dots \sum_{l_{k-1}=0}^n \frac{q^{\sum_{j=1}^{k-1} (i_j(i_j+1))}}{(q, q)_{l_k}^2 \prod_{j=1}^{k-2} (q, q)_{l_j}} \quad (5.36)$$

with $i_j = \sum_{s=j}^{k-1} l_s$. Equations (5.35) and (5.36) yield the result.

2. Substituting ($f = 2k + 1$) in (5.34), we obtain

$$\begin{aligned}
\tilde{J}_{n,K_{2k+1}}(q)/\Delta_n(q) &\doteq_n \sum_{i=0}^n (-1)^i q^{(2k+1)(i+i^2)/2} (q^{-i} - q^{1+i}) \\
&= \sum_{i=0}^n (-1)^i q^{-i/2+i^2/2+ik+i^2k} - \sum_{i=0}^n (-1)^i q^{1+3i/2+i^2/2+ik+i^2k} \\
&= \sum_{i=0}^n (-1)^i q^{-i/2+i^2/2+ik+i^2k} - \sum_{i=1}^n (-1)^i q^{i/2+i^2/2-ik+i^2k}
\end{aligned}$$

Hence

$$\tilde{J}_{n,K_{2k+1}}(q)/\Delta_n(q) \doteq_n f(-q^{2k}, -q) \quad (5.37)$$

Theorem 4.19 implies

$$\tilde{J}_{n,K_{2k+1}}(q)/\Delta_n(q) \doteq_n \frac{1}{\Delta_n(q)} \text{ (diagram of a genus-} k \text{ surface with } 2k \text{ bubbles)} \quad (5.36)$$

However corollary 5.13 implies

$$\frac{1}{\Delta_n(q)} \text{ (diagram of a genus-} k \text{ surface with } 2k \text{ bubbles)} \doteq_n (q, q)_\infty \sum_{l_1=0}^{\infty} \sum_{l_2=0}^{\infty} \dots \sum_{l_{k-1}=0}^{\infty} \frac{q^{\sum_{j=1}^{k-1} (i_j(i_j+1))}}{\prod_{j=1}^{k-1} (q, q)_{l_j}} \quad (5.38)$$

with $i_j = \sum_{s=j}^{k-1} l_s$. Equations (5.37) and (5.38) yield the result. □

References

- [1] G. Glibb and S. Slick, *Propositions equivalent to the Riemann Hypothesis*, Brooklyn Bridge studies in advanced mathematics, **18**, Brooklyn Bridge University Press, 1999.
- [2] G. E. Andrews, and Bruce C. Berndt, *Ramanujan's Lost Notebook: Part I, Volume 1*, Springer, 2005.
- [3] C. Armond, and O. T. Dasbach, *Rogers-Ramanujan Type Identities and the Head and Tail of the Colored Jones Polynomial*, 2011, arXiv:1106.3948v1, preprint.
- [4] C. Armond, *The head and tail conjecture for alternating knots*, 2011, arXiv:1112.3995v1, preprint.
- [5] C. Armond, *Walks along braids and the colored Jones polynomial*, arXiv:1101.3810 (2011), 1-26.
- [6] Bruce C. Berndt, *Ramanujan's notebooks, Part III*, Springer Verlag, New York, 1991.
- [7] O. T. Dasbach and X. Lin, *On the head and the tail of the colored Jones polynomial*, Compositio Mathematica 142 (2006), no. 05, 1332-1342.
- [8] S. Garoufalidis and T. T. Q. Le, *Nahm sums, stability and the colored Jones polynomial*, 2011, arXiv:1112.3905, Preprint.
- [9] S. Garoufalidis and T. Vuong, *Alternating knots, planar graphs and q -series*, 2013, arXiv:1304.1071, Preprint.
- [10] M. Hajij, *The Bubble skein element and applications*, Journal of Knot Theory and Its Ramifications, 2015.
- [11] M. Hajij, *the tail of quantum spin networks*, to appear in Ramanujan Journal, 2015.
- [12] M. Hajij, *The colored kauffman skein relation and the head and tail of the colored jones polynomial*, 2014, arXiv:1401.4537, Preprint.
- [13] V. Huynh and T. T. Q. Le, *On the colored Jones polynomial and the Kashaev invariant*, J. Math. Sci. (N. Y.) 146 (2007), no. 1, 5490-5504.
- [14] Kazuhiro Hikami, *Volume conjecture and asymptotic expansion of q -series*, Experiment. Math. 12, 2003, no. 3, 319-338.
- [15] V.F.R Jones, *A polynomial invariant for knots via von Neumann algebras*, Bull. Amer. Math. Soc. 12 (1985), no. 1 103111.

- [16] V. F. R. Jones, *Index of subfactors*, Invent. Math., 72 (1983), 1-25.
- [17] L. H. Kauffman, *State models and the Jones polynomial*, Topology, 26(1987), 395-401.
- [18] L. H. Kauffman, *An invariant of regular isotopy*, Transactions of the American Mathematical Society 318(2), 1990, pp. 317–371.
- [19] L. Kauffman, and S. Lins, *Temperley-Lieb Recoupling Theory and Invariants of 3-Manifolds*, Princeton Univ. Press, 1994.
- [20] W.B.R. Lickorish, *3-manifolds and the Temperley-Lieb algebra*, Math. Annal, 290:657-670, 1991.
- [21] W.B.R. Lickorish, *The skein method for 3-manifold invariants*, J. Knot Theor. Ramif., 2 (1993), 171-194.
- [22] W.B.R. Lickorish, *An Introduction to Knot Theory*, Springer, 1997.
- [23] J. Laughlin, and A. V. Sills, P. Zimmer, *Rogers-Ramanujan-Slater Type Identities*, Electronic Journal of Combinatorics 15 (2008), no. DS15, 1-59.
- [24] J. Lovejoy, R. Osburn, *The Bailey chain and mock theta functions*, Adv. Math. 238 (2013), 442458.
- [25] G. Masbaum, and P. Vogel, *3-valent graphs and the Kauffman bracket*, Pacific J. Math., 164 (1994), No. 2, 361-381.
- [26] G. Masbaum, *Skein-theoretical derivation of some formulas of Habiro*, Algebraic and Geometric Topology, 3 (2003), 537556.
- [27] S. Morrison, *A formula for the Jones-Wenzl projections*, Unpublished, available at <http://tqft.net/math/JonesWenzlProjections.pdf>.
- [28] K. Murasugi, *Jones polynomials and classical conjectures in knot theory*, Topology 26 (1987), 187-194.
- [29] J.H. Przytycki, *Fundamentals of Kauffman bracket skein module*, Kobe J. Math. 16 (1999), no. 1, 45-66.
- [30] J.H. Przytycki, *Skein modules of 3-manifolds*, Bull. Pol. Acad. Sci. 39(1-2) (1991) 91100.
- [31] V.G. Turaev, *The Conway and Kauffman modules of the solid torus*, Zapiski Nauchnykh Seminarov POMI, 167, 79-89.
- [32] N. Y. Reshetikhin and V. Turaev, *Invariants of three manifolds via link polynomials and quantum groups*, Invent. Math., 103:547-597, 1991.

- [33] M. Thistlethwaite, *Kaufmanns polynomial and alternating links*, Topology 27 (1988), 311-318. 1986.
- [34] V.G. Turaev, *The Conway and Kauffman modules of the solid torus*, Zap. Nauchn. Sem. Lomi 167 (1988), 79-89. English translation: J. Soviet Math. 52, 1990, 2799-2805.
- [35] H. Wenzl, *On sequences of projections*, C. R. Math. Rep. Acad. Sci. Canada, IX (1987), 5-9.
- [36] S. Yamada, *A topological invariant of spatial regular graphs*, Proceeding of Knots 90, De Gruyter 1992, pp. 447-454.

Vita

Mustafa Hajij was born in Damascus City, Syria. He finished his undergraduate studies at Damascus University in 2004. He earned a master of science degree in mathematics from Jordan university for science and technology in 2008. In August 2008 he came to Louisiana State University to pursue graduate studies in mathematics. He is currently a candidate for the degree of Doctor of Philosophy in mathematics, which will be awarded in August 2015.